Natural convection in a horizontal circular cylinder

By SHELDON WEINBAUM

Sperry Rand Research Center, Sudbury, Mass.

(Received 6 August 1963)

In this paper we examine the steady, two-dimensional convective motion which occurs in a horizontal circular cylinder whose wall is non-uniformly heated. One observes several qualitatively different physical phenomena depending on the wall temperature distribution and the value of the Rayleigh number. The low-Rayleigh-number behaviour for the single convective cell heated from below is related to the classical Rayleigh stability problem. The critical Rayleigh number for the single circular cell is approximately five times the value for Rayleigh's multi-cellular configuration. The flow which exhibits a nearly parabolic velocity profile near the critical Rayleigh number, gradually changes to a rigidly-rotating-core behaviour as the Rayleigh number increases. The speed of core rotation is a function of the Prandtl number, whereas the boundary-layer thickness is primarily a function of the Rayleigh number. When the heating is from side to side, the solution shows that as the Rayleigh number increases the core motion is progressively arrested leaving a narrow circulating band of fluid adjacent to the wall. An oblique heating produces a hybrid phenomenon, a low-Rayleigh-number behaviour which is characteristic of the sideways heating case and a high-Rayleigh-number interior motion characteristic of the bottom heating case. To determine the core motion in the high-Rayleigh-number limit, Batchelor's work concerning the uniqueness of incompressible, exactly steady, closed streamline flows with small viscosity is extended to include flows with small thermal conductivity.

1. Introduction

In recent years, because of important heat transfer application in building insulation techniques and nuclear reactor boiler design, special attention has been devoted to natural convection in enclosed spaces in which a single convective cell often appears. Explanations of single-cell convection phenomena, apart from their own intrinsic interest, are important in that they may add to our understanding of multi-cellular motions observed in extended media. The present investigation is concerned with laminar, two-dimensional steady flows inside a horizontal pipe of circular cross-section whose wall is maintained at the sinusoidally-distributed temperature, $T_{\text{wall}} = T_0 + \Delta T \cos(\theta + \phi)$; see figure 1. This family of thermal boundary conditions includes several problems of interest depending on the phase angle, ϕ. With the gravitational field directed as shown, a motionless equilibrium state can exist only when $\phi = \pm \frac{1}{2}\pi$. The configuration with $\phi = \frac{1}{2}\pi$, a fluid heated from below, can be unstable because the density gradient

is positive upward. The phenomena for all other ϕ (of which $\phi = 0$ and $\phi = \frac{1}{4}\pi$ are qualitatively representative) are alike in that motion ensues for all ΔT.

A multi-cellular phenomenon related to our $\phi = \frac{1}{2}\pi$ case was discussed in the literature as early as 1900 when Bénard noted that a fluid contained between two infinite horizontal plates would break up into small convective cells if the lower plane were at a temperature sufficiently higher than the upper one. Bénard reasoned that the viscous forces present at the boundary planes would prevent

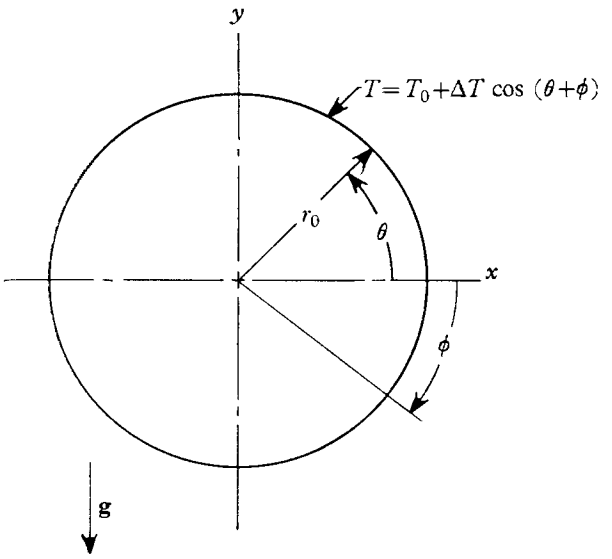

FIGURE 1. Configuration for general problem.

the onset of motion unless the density gradient was steep enough. Lord Rayleigh (1916) showed that this phenomenon is associated with a critical value of the dimensionless Rayleigh number, $\lambda = (\beta g c_p \rho_0^2/\mu k)(r_0^3 \Delta T)$; here μ is the viscosity, k the thermal conductivity, c_p the specific heat, β the coefficient of thermal expansion and ρ_0 the density of the fluid; r_0 and ΔT are one-half the distance and one-half the temperature difference, respectively, between the upper and lower planes. Pellew & Southwell (1940) in their comprehensive linear treatment of the classical Rayleigh stability problem show that $\lambda_{cr} = 106{\cdot}7$. Linear analyses are incapable of predicting the motion at $\lambda > \lambda_{cr}$ for the multi-cellular configuration. Non-linear analyses, such as that of Segel & Stuart (1962), have not yet determined the manner in which the steady state is established or the detailed nature of the final steady motion in the individual cells. Segel & Stuart do give evidence which predicts that the steady-state pattern is, most probably, either an array of long, two-dimensional rectangular roll cells or three-dimensional cells with vertical cell walls whose horizontal cross-sections are regular hexagons.

When convection cells do not have an equilibrium configuration the dependent variables in the governing equations are continuous functions of λ and can be expressed as series expansions in this parameter. Both Batchelor (1954) and Lewis (1950) have determined the first two terms in such series expansions, the former for a single two-dimensional rectangular cell heated from side to side and

the latter for the circular cell with $\phi = 0$. Keeping ϕ arbitrary, we extend Lewis's work to include a rotating inner cylinder whose thermal conductivity is the same as that of the surrounding fluid. In all cases the first two terms are shown to be an adequate approximation to the full series for roughly $\lambda < 10^3$, a Rayleigh number too small for convection to play an important role. With the exception of very slow flows in which $\phi \neq \frac{1}{2}\pi$, any final steady motion will necessitate a consideration of convective mechanisms. Convective effects are very important in any heat-transfer calculation. In this instance Pillow (1952) and Carrier (1953) show with the aid of dimensional analysis, without actually solving the nonlinear conservation equations, that the average Nusselt number for the heat transfer across a convecting cell is proportional to $\lambda^{\frac{1}{4}}$ when λ is large. One must return to the governing equations, however, to evaluate the proportionality constant. The present analysis is the first theory to predict a value which is in good agreement with experimental observations for this constant.

For high values of λ physical reasoning suggests a cell interior in which diffusive processes play an insignificant role. One therefore anticipates a boundary-layer structure, a core that behaves as an inviscid, non-conducting fluid surrounded by a thin layer of fluid adjacent to the wall in which the buoyancy, convection, viscosity and conduction mechanisms are important. The interesting feature of this type of closed-streamline interior flow is that there is no upstream location at which one can prescribe the vorticity and temperature distribution. One has to resort to other means to make such flows determinate. Batchelor (1956) does this for steady incompressible flows by establishing an integral condition governing the vorticity of the interior flow in a simply connected closed region. Specializing to the two-dimensional case, he shows that the vorticity is necessarily a constant for the region contained within the closed streamline at the edge of the boundary layer. Once we have established a similar integral condition to show that the temperature is constant in this same region, we can apply Batchelor's result to our case. The value of the core vorticity is determined by requiring that the viscous boundary-layer flow also be in steady motion. We shall find that an interior with uniform vorticity is not a rigid body core motion when $\phi = 0$. Martini & Churchill (1960) have conducted experiments in the high-Rayleigh-number range for an arrangement similar to our $\phi = 0$ case. Their observations are discussed and compared with the present theory in the concluding section. Solutions for all three cases of interest, $\phi = 0$, $\phi = \frac{1}{4}\pi$, and $\phi = \frac{1}{2}\pi$, which cover the entire λ spectrum are presented.

2. The governing equations

We confine ourselves to motions in which the quadratic and higher-order terms in the velocity can be neglected in the energy equation. This is justifiable if the enthalpy of a fluid element greatly exceeds its kinetic energy. Consequently, we use the governing equations

$$\frac{\partial(\rho u)}{\partial x} + \frac{\partial(\rho v)}{\partial y} = 0, \tag{2.1}$$

$$u\frac{\partial u}{\partial x} + v\frac{\partial u}{\partial y} = -\frac{1}{\rho}\frac{\partial p}{\partial x} + \frac{\mu}{\rho}\left[\nabla^2 u + \frac{1}{3}\frac{\partial}{\partial x}\left(\frac{\partial u}{\partial x} + \frac{\partial v}{\partial y}\right)\right], \tag{2.2}$$

$$u\frac{\partial v}{\partial x}+v\frac{\partial v}{\partial y}=-g-\frac{1}{\rho}\frac{\partial p}{\partial y}+\frac{\mu}{\rho}\left[\nabla^2 v+\frac{1}{3}\frac{\partial}{\partial y}\left(\frac{\partial u}{\partial x}+\frac{\partial v}{\partial y}\right)\right], \tag{2.3}$$

and

$$u\frac{\partial T}{\partial x}+v\frac{\partial T}{\partial y}=\frac{k}{\rho c_p}\nabla^2 T, \tag{2.4}$$

where μ, c_p and k are assumed constant. If the subscript zero denotes conditions at the origin, then the perturbed state (still neglecting quadratic contributions) is given by $\rho/\rho_0 = 1+K(p-p_0)-\beta(T-T_0)$. $K=\rho_0^{-1}(\partial\rho/\partial p)_T$ and $\beta=-\rho_0^{-1}(\partial\rho/\partial T)_p$ are the compressibility and thermal expansion coefficients respectively. It is fundamental for a liquid that $|p_0 K/T_0\beta| \ll 1$, and when the fluid is a gas, we limit our interest to those situations where $|(p-p_0)/p_0| \ll |(T-T_0)/T_0|$. Thus for either a gas or liquid we may write

$$\rho/\rho_0 = 1-\beta(T-T_0). \tag{2.5}$$

If ρ_s, p_s and T_s describe a motionless equilibrium state in which all velocities vanish then $\partial p_s/\partial x = 0$, $\partial p_s/\partial y = -\rho_s g$ and $\nabla^2 T_s = 0$. Only when $\phi = \frac{1}{2}\pi$ is there a non-trivial solution to these last equations which satisfies our thermal boundary condition. The solution for this special case,

$$T_s = T_0-\Delta T(y/r_0), \tag{2.6}$$

represents a fluid with a purely vertical temperature gradient. When $\phi \neq \frac{1}{2}\pi$, we let T_s represent a motionless static state at a uniform temperature, T_0. We express the actual pressure, p, as the sum of the static pressure, p_s, and the incremental pressure, p_i, due to the fluid motion. $\Phi = (T-T_0)/\Delta T$ is a more convenient temperature variable than T. Setting $\gamma = \beta\Delta T$, we combine the buoyancy and pressure terms in (2.3) to obtain

$$-g-\frac{1}{\rho}\frac{\partial p}{\partial y}=-g\left(\frac{\rho-\rho_s}{\rho}\right)-\frac{1}{\rho}\frac{\partial p_i}{\partial y}=\frac{\gamma g}{(1-\gamma\Phi)}\left(\Phi-\frac{T_s-T_0}{\Delta T}\right)-\frac{1}{\rho}\frac{\partial p_i}{\partial y}, \tag{2.7}$$

in which $(T_s-T_0)/\Delta T = -y/r_0$ or 0 depending whether $\phi = \frac{1}{2}\pi$ or $\phi \neq \frac{1}{2}\pi$, respectively. It is convenient to introduce the dimensionless variables

$$U = u/u_0, \quad V = v/u_0, \quad X = x/r_0, \quad Y = y/r_0 \quad \text{and} \quad P = p_i/p_0;$$

the subscript zero implies a convenient reference quantity. r_0, the cylinder radius, is a characteristic length already prescribed for the problem. Two useful scalings are available for each of u_0 and p_0, the preferred pair depending on the method of solution employed. The governing equations are of boundary-layer type when λ is large if $u_0 = (\gamma g r_0)^{\frac{1}{2}}$ and $p_0 = \gamma g \rho_0 r_0$. For general Rayleigh number phenomena a suitable choice is $u_0 = k/\rho_0 c_p r_0$ and $p_0 = k^2/\rho_0 c_p^2 r_0^2$. Equations (2.1), (2.2), (2.3) and (2.4) when expressed in terms of the Prandtl number, $\eta = \mu c_p/k$, and the Rayleigh number, $\lambda = \gamma g c_p \rho_0^2 r_0^3/\mu k$, become

$$\partial U(1+\gamma\Phi)/\partial X + \partial V(1+\gamma\Phi)/\partial Y = 0, \tag{2.8}$$

$$U\frac{\partial U}{\partial X}+V\frac{\partial U}{\partial Y}=-\frac{1}{1-\gamma\Phi}\frac{\partial P}{\partial X}+\left[\left(\frac{\eta}{\lambda}\right)^{\frac{1}{2}},\eta\right]\frac{1}{1-\gamma\Phi}\left[\nabla^2 U+\frac{1}{3}\frac{\partial}{\partial X}\left(\frac{\partial U}{\partial X}+\frac{\partial V}{\partial Y}\right)\right], \tag{2.9}$$

$$U\frac{\partial V}{\partial X}+V\frac{\partial V}{\partial Y}=[1,\eta\lambda]\frac{\Phi-(T_s-T_0)/\Delta T}{1-\gamma\Phi}-\frac{1}{1-\gamma\Phi}\frac{\partial P}{\partial Y}$$
$$+\left[\left(\frac{\eta}{\lambda}\right)^{\frac{1}{2}},\eta\right]\frac{1}{1-\gamma\Phi}\left[\nabla^2 V+\frac{1}{3}\frac{\partial}{\partial Y}\left(\frac{\partial U}{\partial X}+\frac{\partial V}{\partial Y}\right)\right], \tag{2.10}$$

and
$$U\frac{\partial\Phi}{\partial X}+V\frac{\partial\Phi}{\partial Y}=\left[\frac{1}{(\eta\lambda)^{\frac{1}{2}}},1\right]\frac{\nabla^2\Phi}{1-\gamma\Phi}, \tag{2.11}$$

where the coefficients in the brackets depend on which of the foregoing definitions of u_0 and p_0 are used. Equation (2.5) is accurate only when $\Delta T/T_0 \ll 1$. We therefore consider only those situations for which $\gamma\Phi \ll 1$. Introducing the vector description, $\mathbf{V} = U\mathbf{i}+V\mathbf{j}$, we have

$$\operatorname{div}\mathbf{V}=0, \tag{2.12}$$

$$(\mathbf{V}.\nabla)\mathbf{V}=[1,\eta\lambda](\Phi-(T_s-T_0)/\Delta T)\,\mathbf{j}-\nabla P+[(\eta/\lambda)^{\frac{1}{2}},\eta]\nabla^2\mathbf{V} \tag{2.13}$$

and
$$\mathbf{V}.\nabla\Phi=[(\eta\lambda)^{-\frac{1}{2}},1]\nabla^2\Phi, \tag{2.14}$$

where the operators in $(\mathbf{V}.\nabla)\mathbf{V}$ and $\nabla^2\mathbf{V}$ have their usual invariant vector meaning. The wall temperature distribution is prescribed and the velocity vanishes at the wall. Thus, the boundary conditions are

$$U=V=0 \quad\text{and}\quad \Phi=\cos(\theta+\phi) \quad\text{at}\quad r=1. \tag{2.15}$$

By virtue of equation (2.12) a stream-function representation is possible for the velocity. Thus $\mathbf{V}=\operatorname{curl}\Psi\mathbf{k}$, in which $\mathbf{k}$ is a unit vector directed along the cylinder axis. We take the curl of equation (2.13) to eliminate the pressure and write the resulting equations in cylindrical-polar co-ordinates. Since

$$(T_s-T_0)/\Delta T=-Y \quad\text{when}\quad \phi=\tfrac{1}{2}\pi \quad\text{and}\quad \operatorname{curl}Y\mathbf{j}=0,$$

this term vanishes when the curl operation is performed. The governing equations can now be written

$$\left[\left(\frac{\eta}{\lambda}\right)^{\frac{1}{2}},\eta\right]\nabla^2\nabla^2\Psi+\frac{1}{r}\left(\frac{\partial\Psi}{\partial r}\frac{\partial}{\partial\theta}-\frac{\partial\Psi}{\partial\theta}\frac{\partial}{\partial r}\right)\nabla^2\Psi=[1,\eta\lambda]\left(\cos\theta\frac{\partial}{\partial r}-\frac{\sin\theta}{r}\frac{\partial}{\partial\theta}\right)\Phi \tag{2.16a,b}$$

and
$$\left[\frac{1}{(\eta\lambda)^{\frac{1}{2}}},1\right]\nabla^2\Phi+\frac{1}{r}\left(\frac{\partial\Psi}{\partial r}\frac{\partial}{\partial\theta}-\frac{\partial\Psi}{\partial\theta}\frac{\partial}{\partial r}\right)\Phi=0, \tag{2.17a,b}$$

where $V_r=(1/r)\,\partial\Psi/\partial\theta$ and $V_\theta=-\partial\Psi/\partial r$ are the radial and tangential velocity components. Equations (2.16) and (2.17) together with the boundary conditions,

$$\partial\Psi/\partial r=\partial\Psi/\partial\theta=0 \quad\text{and}\quad \Phi=\cos(\theta+\phi) \quad\text{at}\quad r=1,$$

complete the statement of the problem.

3. Very slow flows for $\phi \neq \frac{1}{2}\pi$

We first consider motions in the 'Stokes flow' régime where all perturbations are so small that the quadratic terms in the momentum equation are unimportant. There is no boundary layer, and momentum transfer, even in the cell interior, is not strongly influenced by convection. For a first approximation we express the convective contribution in the energy equation by $\mathbf{V}.\nabla\Phi_s$. When $\phi \neq \frac{1}{2}\pi$, $\mathbf{V}.\nabla\Phi_s=0$, but for $\phi=\frac{1}{2}\pi$, $\mathbf{V}.\nabla\Phi_s=-V_y$. We exclude the $\phi=\frac{1}{2}\pi$ case here and consider this special configuration separately in §5. Equations (2.16*b*) and (2.17*b*) linearized in the above fashion become

$$\nabla^2\nabla^2\Psi=\lambda\left(\cos\theta\frac{\partial\Phi}{\partial r}-\frac{\sin\theta}{r}\frac{\partial\Phi}{\partial\theta}\right) \tag{3.1}$$

and
$$\nabla^2\Phi=0. \tag{3.2}$$

With little extra labour, we can extend the 'Stokes flow' solutions to include a rotating solid inner cylinder whose thermal conductivity is the same as that of the surrounding fluid. If the dimensionless radius of this solid core is 'a' and rotates with angular velocity ω, then the appropriate boundary conditions are

$$\left.\begin{aligned} &V_r = V_\theta = 0, \quad \Phi = \cos(\theta+\phi) \quad \text{at} \quad r = 1 \\ \text{and} \quad &V_r = 0, \quad V_\theta = \omega a, \quad \Phi = a\cos(\theta+\phi) \quad \text{at} \quad r = a, \end{aligned}\right\} \tag{3.3}$$

with the additional requirement that V_r, V_θ, Φ and P be periodic in θ.

The resulting solutions for the temperature, velocity components and incremental pressure are

$$\Phi = r\cos(\theta+\phi), \tag{3.4}$$

$$V_r = 0, \quad V_\theta = \frac{\omega a^2}{a^2-1}\left(r-\frac{1}{r}\right)+\frac{\lambda\cos\phi}{16}\left[-\frac{a^2}{r}+(a^2+1)r-r^3\right], \tag{3.5}$$

and

$$P = \tfrac{1}{2}\eta\lambda r^2\sin\theta\cos(\theta+\phi), \tag{3.6}$$

respectively. Two results are of interest in the foregoing linearized theory. The velocity is of a purely tangential nature, $V_r = 0$, the streamlines being circles concentric about the origin, and the pressure is unaffected by the rotation of the inner cylinder. The former is a consequence of the fact that the driving term on the right-hand side of equation (3.1) is independent of θ. If the inner cylinder experiences a zero net moment it will rotate with a constant angular velocity. The shear stress at any point on the cylinder surface is given by

$$\tau_{r\theta} = \left(\frac{\partial V_\theta}{\partial r}-\frac{V_\theta}{r}+\frac{1}{r}\frac{\partial V_r}{\partial\theta}\right)_{r=a}.$$

Since $\tau_{r\theta}$ is independent of θ we can replace the zero torque condition,

$$\int_0^{2\pi}\tau_{r\theta}\,a\,d\theta = 0,$$

by simply $\tau_{r\theta}|_{r=a} = 0$. From equation (3.5) this last requirement is fulfilled when

$$\omega = \tfrac{1}{16}\lambda(a^2-1)^2\cos\phi. \tag{3.7}$$

A fluid and a solid core are not interchangeable. The motion in a fluid core is given by $V_\theta = \frac{1}{16}\lambda\cos\phi\,(r-r^3)$, as is apparent from equation (3.5) if we let $a \to 0$, and is not a rigid-body rotation.

4. Low-Rayleigh-number expansions

As previously mentioned, the existence of motion for all λ when $\phi \neq \frac{1}{2}\pi$ gives credence to the conjecture that with the exception of the special case $\phi = \frac{1}{2}\pi$, Φ and Ψ are smooth functions of λ and as such can be developed in power series in this parameter. Since the evaluation of more than the first two terms of such series is laborious, the usefulness of this method of solution, potentially valid for all λ, is limited to situations in which λ is sufficiently small for these first two terms to be a good approximation for the series summations. Thus,

$$\left.\begin{aligned} \Phi &= \Phi_0+\Phi_1\lambda+\ldots, \\ \Psi &= \Psi_1\lambda+\Psi_2\lambda^2+\ldots, \end{aligned}\right\} \tag{4.1}$$

where we have no prior knowledge as to how quickly these series converge. From equations (2.16*b*) and (2.17*b*), the usual separation in powers of λ leads to the following set of equations:

$$\nabla^2\Phi_0 = 0, \tag{4.2a}$$

$$\nabla^2\Phi_1 + \frac{1}{r}\left(\frac{\partial\Psi_1}{\partial r}\frac{\partial}{\partial\theta} - \frac{\partial\Psi_1}{\partial\theta}\frac{\partial}{\partial r}\right)\Phi_0 = 0, \tag{4.2b}$$

$$\nabla^2\nabla^2\Psi_1 = \left(\cos\theta\frac{\partial}{\partial r} - \frac{\sin\theta}{r}\frac{\partial}{\partial\theta}\right)\Phi_0, \tag{4.2c}$$

$$\eta\nabla^2\nabla^2\Psi_2 + \frac{1}{r}\left(\frac{\partial\Psi_1}{\partial r}\frac{\partial}{\partial\theta} - \frac{\partial\Psi_1}{\partial\theta}\frac{\partial}{\partial r}\right)\nabla^2\Psi_1 = \eta\left(\cos\theta\frac{\partial}{\partial r} - \frac{\sin\theta}{r}\frac{\partial}{\partial\theta}\right)\Phi_1. \tag{4.2d}$$

If we consider the problem with the inner cylinder present, the boundary conditions on the coefficients are

$$\left.\begin{aligned} &\Phi_0 = \cos(\theta+\phi), \quad \Phi_1 = \frac{\partial\Psi_1}{\partial r} = \frac{\partial\Psi_2}{\partial r} = \frac{\partial\Psi_1}{\partial\theta} = \frac{\partial\Psi_2}{\partial\theta} = 0 \quad \text{at} \quad r = 1 \\ \text{and} \quad &\Phi_0 = a\cos(\theta+\phi), \quad \frac{\partial\Psi_1}{\partial r} = -\frac{\omega a}{\lambda}, \quad \Phi_1 = \frac{\partial\Psi_1}{\partial\theta} = \frac{\partial\Psi_2}{\partial r} = \frac{\partial\Psi_2}{\partial\theta} = 0 \\ &\qquad\qquad\qquad\qquad\qquad\qquad\qquad\qquad\qquad\qquad \text{at} \quad r = a. \end{aligned}\right\} \tag{4.3}$$

ω will be of order λ if the motion of the inner cylinder is a free convection phenomenon and not a forced rotation. All dependent variables must, of course, be continuous at $\theta = 0$ and 2π.

The solutions for Φ_0 and Ψ_1 are just the Stokes flow solutions obtained in § 3, $\Phi_0 = r\cos(\theta+\phi)$ and

$$\Psi_1 = \frac{\omega a^2}{2\lambda(1-a^2)}r^2\ln r + \frac{\cos\phi}{16}\left[a^2\ln r - \frac{a^2+1}{2}r^2 + \frac{r^4}{4}\right]. \tag{4.4}$$

Equations (4.2*b*) and (4.2*d*) are reduced to constant-coefficient equations when we introduce the independent-variable transformation, $\xi = \ln r$. The solution for Φ_1 is

$$\begin{aligned}\Phi_1 = \Bigg\{&\left(\frac{\omega a^2}{2\lambda(a^2-1)} + \frac{a^2\cos\phi}{32}\right)\left[r\left(\frac{1}{4} - \frac{r^2}{4} + \ln r\right)\left(\frac{a^2\ln r}{a^2-1} - \frac{a^2}{4}\right)\left(\frac{1}{r} - r\right)\right] \\ &+ \frac{\cos\phi}{384}\left[r^5 - 3r^3 - r(a^4 - 2a^2 - 2) + \frac{a^2(a^2-2)}{r}\right]\Bigg\}\sin(\theta+\phi).\end{aligned} \tag{4.5}$$

The solution for Ψ_2 is very lengthy in the general case that includes the rotation of an inner cylinder and is omitted here; it is shown in detail in the author's thesis (Weinbaum 1963). However, with ϕ still arbitrary, a relatively simple expression is available for Ψ_2 in the limiting case, $a \to 0$, namely,

$$\begin{aligned}\Psi_2 = &\frac{\sin 2\phi}{(768)^2}(-28r^2 + 24r^4 - 8r^6 + r^8) \\ &- \frac{\cos\phi\sin(2\theta+\phi)}{768\,(960)}(11r^2 - 24r^4 + 15r^6 - 2r^8) + \text{const.}\end{aligned} \tag{4.6}$$

If the foregoing solutions are to be applied meaningfully to a practical situation, we must estimate the maximum value of λ for which the first two terms of

the series expansions are adequate approximations to the complete summations. One crude criterion to provide such a value is to require the ratio of the maximum values of the first two terms of the series be roughly unity. Based for simplicity on the case where the inner cylinder is absent, this occurs when $\lambda < 600$ and $\lambda < 20{,}000$ in the series expansions for Φ and Ψ', respectively, either of which is a very small Rayleigh number in most practical applications. This is not to say that the series for Φ and Ψ' will not converge for values of λ exceeding those above, but rather that too many terms are required for the series representation in (4.1) to be practicable. In summary, the usefulness of this series expansion method is confined to problems wherein conduction as opposed to convection is the dominant means of energy transfer.

5. The critical Rayleigh number for the $\phi = \frac{1}{2}\pi$ case

It is known from linear analyses mentioned earlier that the viscous stress in the neighbourhood of the boundary prevent the onset of motion in the Rayleigh stability problem unless $\lambda > 106{\cdot}7$. For a single circular cell heated from below, one intuitively expects a higher critical Rayleigh number than the preceeding value for Rayleigh's multi-cellular configuration since the side walls are not shearless, as is the case in the problem Rayleigh treated. The perturbation velocities accompanying the onset of motion are small. Therefore, we use the same approximations discussed in §3 for very slow viscous flows when $\phi \neq \frac{1}{2}\pi$. Here $\mathbf{V}.\nabla\Phi_s = \partial\Psi'/\partial X$ so that instead of (3.1) and (3.2) we now have

$$\nabla^2\nabla^2\Psi' = \lambda(\partial\Phi/\partial X) \quad \text{and} \quad \nabla^2\Phi - \partial\Psi'/\partial X = 0. \tag{5.1}$$

These last two equations combine to give a sixth-order homogeneous equation for Ψ',

$$\nabla^2\nabla^2\nabla^2\Psi' - \lambda(\partial^2\Psi'/\partial X^2) = 0. \tag{5.2}$$

A simple Fourier analysis is not easily applied to the single circular cell since the driving term, $\lambda(\partial^2\Psi'/\partial X^2)$, does not have a simple form when expressed in cylindrical polar co-ordinates. The variational problem equivalent to equation (5.2) and its accompanying boundary conditions is to determine that special Ψ', satisfying the same boundary conditions, for which the integral

$$I = \frac{1}{2}\int_{-1}^{1}\int_{-(1-X^2)^{\frac{1}{2}}}^{(1-X^2)^{\frac{1}{2}}}\left[\left(\frac{\partial^3\Psi'}{\partial X^3}\right)^2 + 3\left(\frac{\partial^3\Psi'}{\partial X^2\partial Y}\right)^2 + 3\left(\frac{\partial^3\Psi'}{\partial X\partial Y^2}\right)^2 + \left(\frac{\partial^3\Psi'}{\partial Y^3}\right)^2 - \lambda\left(\frac{\partial\Psi'}{\partial X}\right)^2\right]dX\,dY \tag{5.3}$$

is stationary in value. We conjecture that it is possible to represent closely that Ψ' for which I is stationary by a finite series of terms, say $\Psi'(r,\theta) = \sum_{n=1}^{N} A_n f_n(r,\theta)$. This approximate Ψ' must satisfy the boundary conditions,

$$\partial\Psi'/\partial r = \partial\Psi'/\partial\theta = 0 \quad \text{at} \quad r = 1,$$

be bounded everywhere, and be single-valued at the origin. Provided the velocities do not vary rapidly anywhere in the cell, a prospect which is unlikely at small Rayleigh numbers since viscous stresses play an important role everywhere and would damp out any rapid fluctuations, a polynomial of small degree in

n and independent of θ should be an adequate first approximation for Ψ. As a first guess we try

$$\Psi = A_1(r^2 - \tfrac{1}{2}r^4) = A_1[X^2 + Y^2 - \tfrac{1}{2}(X^2 + Y^2)^2], \tag{5.4}$$

which obeys all the requirements specified in the penultimate sentence.

Substituting this approximation for Ψ in (5.3) and performing the double integration we find $I = 48\pi A_1^2(1 - \lambda/576)$; if I is to be a minimum, $\partial I/\partial A_1 = 0$, and $\lambda_{cr} = 576$. An apparent refinement on the present solution that gives credence to the accuracy of the result just obtained for λ_{cr} is to take account of the angular dependence in the representation of Ψ. An improved approximation for the stream function which fulfils all the forementioned conditions is

$$\Psi = A_1 r^2(1 - \tfrac{1}{2}r^2) + A_2 r^2(1-r)^2 \sin 2\theta + A_3 r^2(1-r)^2 \cos 2\theta. \tag{5.5}$$

The same procedure now leads to a third-order determinantal equation for λ whose smallest positive root has the value $\lambda = 576{\cdot}62$. In view of the close agreement of this last value with that of the first result, there is good reason to believe that further refinements would not yield values for λ_{cr} very different from those already obtained. Thus, the critical Rayleigh number for the single circular cell is roughly five times the value for Rayleigh's multicellular configuration.

6. The high-Rayleigh-number interior motion

It is well known that the thickness of the region of thermal influence adjacent to a solid boundary decreases as the Rayleigh number increases in laminar free-convection phenomena. For large λ, the thickness of this thermal layer is small compared to the radius of the convection cell, and in the limit, $\lambda \to \infty$, such a layer becomes a singular surface. In the interior region, where the relative importance of diffusive processes is slight, the flow essentially obeys the inviscid fluid equations which in the steady state require the temperature to be constant along a streamline and similarly the vorticity if the streamlines lie entirely within a constant temperature region. Non-conducting, frictionless flows outside a boundary layer are usually made unique by imposing boundary conditions that specify the temperature and vorticity distribution at infinity; however, no such boundary conditions are available for cavity flows with closed streamlines. Therefore, we must first establish the necessary conditions which make the interior flow determinate, then obtain interior solutions satisfying these conditions, and lastly determine the lower limit on λ for which the assumed boundary-layer structure exists. The first two points we consider here; the third we answer in § 10.

As $\lambda \to \infty$ the most highly differentiated terms in equations (2.16a) and (2.17a) become negligible everywhere except in the immediate vicinity of the boundary where their presence is essential if the boundary conditions at $r = 1$ are to be satisfied. The interior flow conforms to the so-called 'core equations',

$$\frac{\partial \Psi}{\partial r}\frac{\partial \Phi}{\partial \theta} - \frac{\partial \Psi}{\partial \theta}\frac{\partial \Phi}{\partial r} = 0 \quad \text{and} \quad -\frac{1}{r}\left(\frac{\partial \Psi}{\partial r}\frac{\partial}{\partial \theta} - \frac{\partial \Psi}{\partial \theta}\frac{\partial}{\partial r}\right)\omega = \left(\cos\theta\frac{\partial}{\partial r} - \frac{\sin\theta}{r}\frac{\partial}{\partial \theta}\right)\Phi, \tag{6.1}$$

in which $\omega = -\nabla^2\Psi$ is the vorticity. Pillow (1952) showed that

$$\Phi = F(\Psi) \quad \text{and} \quad \omega = -YF'(\Psi) + G(\Psi) \tag{6.2}$$

are general solutions to (6.1), where F and G are arbitrary. Temperature gradients, in general, generate vorticity whether or not diffusive mechanisms are present. Batchelor (1956) has shown for steady, incompressible flows that the contribution from viscous forces to the rate of change of circulation around any closed streamline lying entirely within the core region is identically zero no matter how small the viscosity may be. Mathematically stated,

$$\oint \nabla \times \boldsymbol{\omega} . \mathbf{ds} = 0 \quad \text{if} \quad \mu \neq 0. \tag{6.3}$$

For two-dimensional closed-streamline flows this condition can be combined with (6.2), if $F'(\Psi) = 0$ and $\Phi = \text{const.}$, to show that the vorticity is uniform in a simply connected region with small but non-zero, viscous forces.

Consider a volume, V, whose surface, A, is fixed in space. An energy balance applied to this volume requires that

$$\frac{\partial}{\partial t}\int_V \rho(e + \tfrac{1}{2}q^2)\, d\tau = -\int_A \rho(e + \tfrac{1}{2}q^2)\, \mathbf{V} . \mathbf{n} dA - \int_A p\mathbf{V} . \mathbf{n} dA + \int_A \boldsymbol{\tau} . \mathbf{n} dA + \int_V \rho \mathbf{g} . \mathbf{V} d\tau - \int_A k \nabla T . \mathbf{n} dA, \tag{6.4}$$

where the symbols have their usual meaning and $\mathbf{n}$ is a unit outward normal vector. If the flow is steady, the integral on the left-hand side of equation (6.4) vanishes. The first two integrals on the right-hand side likewise vanish if we choose A to coincide with a stream surface, since $\mathbf{V} . \mathbf{n} = 0$ at such a surface. In general, energy changes taking place in a fluid element due to the action of buoyancy and viscous forces are higher-order effects in free convection problems. Therefore, the integral condition,

$$\int_A \nabla T . \mathbf{n} dA = 0, \tag{6.5}$$

must be satisfied on every closed stream surface since $k \neq 0$, although it may be arbitrarily small. We consider now the two-dimensional flow in a region where each μ and k are small, hence the solutions in (6.2) valid. ∇T and $\mathbf{n}$ are everywhere parallel if A lies entirely within a region where diffusive processes are unimportant. Since $d\Psi/q$ is the displacement corresponding to an increment $d\Psi$ in Ψ, condition (6.5) can be written as

$$\frac{dT}{d\Psi}\int_A q dA = 0. \tag{6.6}$$

Unless the integral vanishes, in which event q is identically zero, $dT/d\Psi = 0$. Thus, the temperature distribution is uniform in the interior and, consequently, the vorticity distribution too. It appears that two-dimensional, closed-streamline flow at high λ cannot be steady until the persistent effect of diffusive pro-

cesses has eventually evened out any variation of temperature and vorticity that may have been present initially in the interior.

The equations governing the flow, (2.16) and (2.17), and the boundary conditions require that Φ change sign on reflexion about the origin whereas ω and Ψ' are centro-symmetric. As a result, $\Phi = 0$ in the core. ω_0, the value of the vorticity in the interior, is determined by requiring the boundary-layer flow also to be in steady motion. This occurs when the buoyancy couple present in the boundary layer just balances the resisting torque exerted on the fluid by the wall. Both moments must cancel if the core is to rotate with a constant angular velocity. An interesting special case occurs when the core motion ceases, and $\omega_0 = 0$. This curious phenomenon does happen for our $\phi = 0$ configuration. In the general case the core stream function, Ψ'_0, satisfies Poisson's equation $\nabla^2\Psi'_0 = \omega_0$, whose general periodic solution for a circular geometry is given by

$$\Psi'_0 = -\tfrac{1}{4}\omega_0 r^2 + \sum_{m=1}^{\infty} A_m r^m e^{im\theta}; \tag{6.7}$$

the A_m are constants whose exact values are determined by matching the solutions for the core and boundary-layer flows.

7. An approximate solution of the boundary-layer equations for the $\phi = \frac{1}{2}\pi$ case

Neither the interior solution for the temperature distribution nor the stream function satisfy the boundary conditions at $r = 1$. In accordance with usual boundary-layer theory, we anticipate that when λ is large the solutions for Φ and Ψ' have the form

$$\Phi = \Phi_0 + \Phi_1 \quad (\Phi_0 = 0) \quad \text{and} \quad \Psi' = \Psi'_0 - \epsilon^{-a}\Psi'_1 \quad (a < 0), \tag{7.1}$$

where $\epsilon = (\eta\lambda)^{-\frac{1}{2}}$ and a is an unspecified negative constant whose exact value is determined by requiring that all mechanisms, buoyancy, viscosity, conduction, and convection, be important in the boundary-layer region. Since $\partial\Psi'/\partial\theta = 0$ at the wall, $\partial\Psi'_0/\partial\theta = \epsilon^{-a}(\partial\Psi'_1/\partial\theta)$ at $r = 1$. $\partial\Psi'_1/\partial\theta$ is of order unity for conditions are changing rapidly only in the direction perpendicular to the boundary. Thus $\partial\Psi'_0/\partial\theta$ is of order ϵ^{-a}, and the coefficients, A_m, in equation (6.7) must also be of this order. Unless ω_0 is of order ϵ^{-a} or smaller, the interior flow is basically a solid core rotation, and the velocity at the edge of the boundary layer is closely approximated by $\mathbf{V} = \frac{1}{2}\omega_0\boldsymbol{\theta}$, if the boundary-layer thickness, δ, is $\ll 1$.

In view of the preceding discussion, equations (2.16a) and (2.17a) have the asymptotic form

$$\eta\epsilon\nabla^2\nabla^2\Psi' - \frac{\omega_0}{2}\frac{\partial\nabla^2\Psi'}{\partial\theta} = \left(\cos\theta\frac{\partial}{\partial r} - \sin\theta\frac{\partial}{\partial\theta}\right)\Phi \tag{7.2}$$

and

$$\epsilon\nabla^2\Phi - \frac{\omega_0}{2}\frac{\partial\Phi}{\partial\theta} = 0, \tag{7.3}$$

for the flow at the edge of the boundary layer. These equations are a classical Oseen linearization of the equations describing the boundary-layer flow. In cases where the free-stream velocity is not influenced by processes taking place

in the boundary layer, such as the steady flow past a semi-infinite flat plate, the solution of the classical Oseen equations will describe correctly the far-field behaviour at the edge of the boundary layer. This same solution will not continue to be the correct value in the slow flow region just adjacent to the wall since the equations are integrated through an intermediate region in which this simple linearization overestimates the convective contribution. In dealing with closed-streamline flows, one needs a more subtle Oseen-type linearization, for the interior behaviour does depend on the boundary-layer flow with the result that the classical Oseen solution provides a poor description everywhere. An improvement on the classical Oseen theory which eliminates some of the foregoing contradiction and corroborates better with experimentally measured heat-transfer rates is based on Carrier's (1953) hypothesis that it is a closer adherence to physical reality if, instead of using zero as in the Stokes theory or $\frac{1}{2}\omega_0$ as in the Oseen method, we choose for the linearizing velocity a constant, c, falling somewhere between these two limits whose exact value is determined afterwards by a judicious averaging process consistent with proper overall momentum or energy transport. There is still no assurance that a solution which exhibits the right behaviour in the near field will continue to the correct behaviour in the far field, or vice versa; however, we hope a wise averaging procedure for these convective terms will reduce to a minimum the differences between the exact and linearized solutions.

The boundary-layer terms, Φ_1 and Ψ_1, will be smooth functions of their arguments if we stretch the co-ordinate perpendicular to the boundary; the co-ordinate parallel to its length need not be scaled. Such a co-ordinate stretching is

$$\xi = (1-r)\,\epsilon^a \quad (a < 0), \tag{7.4}$$

where, if we identify the a above with the a used in (7.1), $\partial\Phi_1/\partial\xi$ and $\partial\Psi_1/\partial\xi$ are of order unity. Subsequently, we shall refer to the governing equations when $\frac{1}{2}\omega_0$ is used for the linearizing velocity as the Oseen formulation and when c is used as the 'modified Oseen' formulation. In the scaled co-ordinate system we have, to order ϵ^a,

$$\eta\epsilon^{1+2a}\,\partial^4\Psi_1/\partial\xi^4 - (\tfrac{1}{2}\omega_0, c)\,\partial^3\Psi_1/\partial\xi^2\partial\theta = \cos\theta\,\partial\Phi_1/\partial\xi \tag{7.5}$$

and

$$\epsilon^{1+2a}\,\partial^2\Phi_1/\partial\xi^2 - (\tfrac{1}{2}\omega_0, c)\,\partial\Phi_1/\partial\theta = 0, \tag{7.6}$$

where $a = -\frac{1}{2}$ if all terms play a significant role. Similarly, our boundary conditions become when we specialize to $\phi = \frac{1}{2}\pi$

$$\Phi_1 = -\sin\theta, \quad \frac{\partial\Psi_1}{\partial\theta} = \epsilon^{-\frac{1}{2}} \sum_{m=1}^{\infty} imA_m e^{im\theta}, \quad \frac{\partial\Psi_1}{\partial\xi} = \tfrac{1}{2}\omega_0 - \sum_{m=1}^{\infty} mA_m e^{im\theta}$$

$$\text{at} \quad \xi = 0 \quad \text{and} \quad \Phi_1 = \Psi_1 = 0 \quad \text{at} \quad \xi = \infty. \tag{7.7}$$

Equations (7.5) and (7.6) with boundary conditions (7.7) are expediently solved in polar complex-variable notation using a standard separation-of-variables procedure. For the classical Oseen case the real parts of these solutions are

$$\Phi = -\exp\{(r-1)\,(\tfrac{1}{8}\lambda)^{\frac{1}{4}}\}\sin[\theta + (r-1)\,(\tfrac{1}{8}\lambda)^{\frac{1}{4}}] \tag{7.8}$$

and
$$\Psi = -\sqrt{\frac{2}{\eta}}\left(\frac{r^2}{4}\right)\left[1+\left(\frac{8}{\lambda}\right)^{\frac{1}{4}}\frac{\eta^{\frac{3}{2}}}{\eta-2}\cos(2\theta+\tfrac{3}{4}\pi)\right]$$
$$+\frac{1}{(8\lambda)^{\frac{1}{4}}}\left\{\frac{\eta}{\eta-2}\exp\{(r-1)(\tfrac{1}{2}\eta^2\lambda)^{\frac{1}{4}}\}\cos[(r-1)(\tfrac{1}{2}\eta^2\lambda)^{\frac{1}{4}}+2\theta+\tfrac{3}{4}\pi]\right.$$
$$-\sqrt{\frac{2}{\eta}}\exp\{(r-1)(\lambda/8)^{\frac{1}{4}}\}\left[\cos[(r-1)(\lambda/8)^{\frac{1}{4}}+\tfrac{3}{4}\pi]\right.$$
$$\left.\left.+\frac{\eta}{\eta-2}\cos[(r-1)(\lambda/8)^{\frac{1}{4}}+2\theta+\tfrac{3}{4}\pi]\right]\right\}; \tag{7.9}$$

thus, the core vorticity adjusts to the value $\omega_0 = (2/\eta)^{\frac{1}{2}}$ when the boundary-layer flow is in steady motion. The corresponding solutions based on the 'modified Oseen' linearization are

$$\Phi = -\exp\{\tfrac{1}{2}c(r-1)(\eta\lambda)^{\frac{1}{4}}\}\sin[\theta+(\tfrac{1}{2}c)^{\frac{1}{2}}(r-1)(\eta\lambda)^{\frac{1}{4}}] \tag{7.10}$$

and
$$\Psi = -\frac{r^2}{4\eta c}\left[1-\frac{\eta}{\eta-2}\left(\frac{\eta}{c^2\lambda}\right)^{\frac{1}{4}}\left(\frac{2}{\sqrt{\eta}}-\sqrt{2}\right)\cos(2\theta+\tfrac{3}{4}\pi)\right]$$
$$-\frac{1}{2c^{\frac{3}{2}}(\eta\lambda)^{\frac{1}{4}}}\left\{-\sqrt{\frac{\eta}{2}}\left(\frac{1}{\eta-2}\right)\exp\{\sqrt{c}(r-1)(\lambda/\eta)^{\frac{1}{4}}\}\cos[\sqrt{c}(r-1)(\lambda/\eta)^{\frac{1}{4}}+2\theta+\tfrac{3}{4}\pi]\right.$$
$$+\frac{1}{\eta}\exp\{(\tfrac{1}{2}c)^{\frac{1}{2}}(r-1)(\eta\lambda)^{\frac{1}{4}}\}\left[\cos\{(\tfrac{1}{2}c)^{\frac{1}{2}}(r-1)(\eta\lambda)^{\frac{1}{4}}+\tfrac{3}{4}\pi\}\right.$$
$$\left.\left.+\frac{\eta}{\eta-2}\cos\{(\tfrac{1}{2}c)^{\frac{1}{2}}(r-1)(\eta\lambda)^{\frac{1}{4}}+2\theta+\tfrac{3}{4}\pi\}\right]\right\}, \tag{7.11}$$

where c is still to be determined. This improved solution shows that the core rotates with a constant angular velocity, hence experiences a zero net torque, when $\omega_0 = 1/\eta c$.

There are several physically meaningful averaging processes for determining the constant c. The obvious possibility, demanding that the difference between the linearized convective terms in equations (7.5) or (7.6) and their non-linearized counterparts vanish when averaged over all (ξ, θ)-space, fails in the present case. Due to the opposing periodicity properties of Φ and Ψ the c-dependence cancels out when the θ integration is performed. A lengthier, but probably more accurate scheme is to substitute our approximate solutions in the non-linear equations governing the boundary-layer flow and require that their integrated average over all (ξ, θ)-space be zero. However, the θ-integration again leads to the same difficulty. We, therefore, weight the exact equations with a function of θ that picks out the angular behaviour of the solutions. $\cos\theta$ is appropriate for the thermal equation since Φ is anti-symmetric, whereas $\cos 2\theta$ is suitable for the momentum equation since Ψ is centro-symmetric. Either evaluation is laborious, and the values for c obtained from each should not differ by much. We choose the averaging procedure which uses the thermal equation, that is

$$\int_0^\infty\int_0^{2\pi}\left[\frac{\partial^2\Phi}{\partial\xi^2}-\left(\frac{\omega_0}{2}-\frac{\partial\Psi_1}{\partial\xi}\right)\frac{\partial\Phi}{\partial\theta}+\left\{\epsilon^{-\frac{1}{2}}\left(\frac{\partial\Psi_0}{\partial\theta}\right)_{r=1}-\frac{\partial\Psi_1}{\partial\theta}\right\}\frac{\partial\Phi}{\partial\xi}\right]\cos\theta\,d\theta\,d\xi = 0, \tag{7.12}$$

since it is by far the shorter of the two. Both the θ and ξ integrations can be performed analytically. The result is a quadratic equation for c whose physically possible root is

$$c = \frac{1}{\sqrt{\eta}}\left[\frac{1}{8} + \frac{1-(\frac{1}{2}\eta)^{\frac{1}{2}}}{2\eta(1-4/\eta^2)}\right]^{\frac{1}{2}}. \tag{7.13}$$

Thus the vorticity in the cell interior adjusts in the steady state to the value

$$\omega_0 = \frac{1}{\sqrt{\eta}}\left[\frac{1}{8} + \frac{1-(\frac{1}{2}\eta)^{\frac{1}{2}}}{2\eta(1-4/\eta^2)}\right]^{-\frac{1}{2}}. \tag{7.14}$$

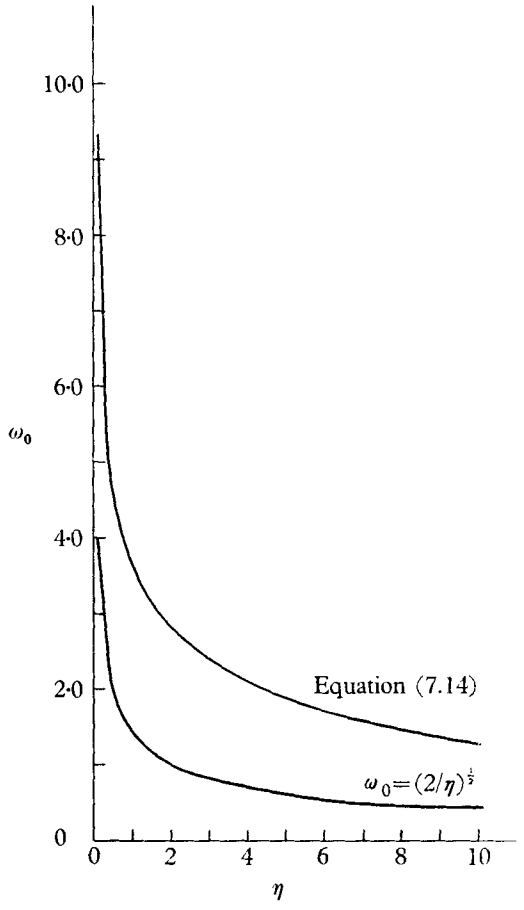

FIGURE 2. Core vorticity as a function of Prandtl number, $\phi = \frac{1}{2}\pi$ and λ large.

Equation (7.14) and the classical Oseen result, $\omega_0 = (2/\eta)^{\frac{1}{2}}$, are plotted in figure 2. For most gases, Prandtl numbers fall within the range $0{\cdot}6 < \eta < 0{\cdot}8$ and for most liquids $0{\cdot}9 < \eta < 7{\cdot}0$. These limits include a wide range of temperatures and pressures. In general, the 'modified Oseen' theory predicts core velocities which are at least a factor of two greater than the corresponding classical Oseen result. Since $t = r_0/u_0 = (r_0/\beta g \Delta T)^{\frac{1}{2}}$ is the characteristic time of the problem, the actual vorticity, ω_{OD}, can be written $\omega_{OD} = \omega_O(\beta g \Delta T/r_0)^{\frac{1}{2}}$. Whereas the Rayleigh number is the significant parameter in determining the boundary-layer thickness, the Prandtl number is the governing parameter in determining the

angular velocity of the core. Based on the 'c/r' solution presented in § 8, solutions for the maximum velocity derived from equation (7.11) are accurate to within 10% for $\eta\lambda > 5 \times 10^4$. Temperature and velocity profiles are discussed in § 10.

Perhaps the best illustration of the power of the 'modified Oseen' technique in the present problem is the reasonable agreement its results exhibit when compared with empirically measured heat-transfer rates. The average Nusselt number, N, for the heat transfer across the upper half of the cell wall is given by

$$N = \frac{hr_0}{k} = \frac{1}{\pi}\int_0^\pi \left(\frac{\partial \Phi}{\partial r}\right)_{r=1} d\theta. \tag{7.15}$$

Experimentally, Schmidt & Saunders (1937) found that the heat transfer across two horizontal plates is represented by $N = 0{\cdot}23\lambda^{\frac{1}{4}}$. Our solutions for Φ, equations (7.8) and (7.10), predict $N = 0{\cdot}351\lambda^{\frac{1}{4}}$ and $N = 0{\cdot}236\lambda^{\frac{1}{4}}$ for the classical Oseen and 'modified Oseen' analyses, respectively. These results are for a unit Prandtl number.

8. The 'c/r' solution

The linearized Oseen boundary-layer method just shown for the $\phi = \frac{1}{2}\pi$ case fails when $\phi = 0$, for a rigid-core rotation is not compatible with any steady boundary-layer flow. We seek a simplifying reformulation of equations (2.16) and (2.17) which requires no further information about the cell interior other than that core temperature and vorticity are uniform. The non-linear terms, $\mathbf{V}.\nabla\Phi$ and $\mathbf{V}.\nabla\omega$, which are the major source of mathematical difficulty, are essentially zero in the core when λ is large since Φ and ω are each constant in this region. At the other end of the λ-spectrum, the slow-flow régime, convective mechanisms are unimportant everywhere within the cell because all velocities are very small. The absence of a radial velocity component in the Stokes-flow solution and the intuitive notion of a continuous velocity boundary layer with a uni-directional motion (no stagnation point) in the high-λ limit together suggest a flow which is basically θ-directed everywhere for all λ. Thus, for a first approximation, we neglect the θ-dependence and introduce the linearizing velocity, $\mathbf{V} = c(\lambda)f(r)\boldsymbol{\theta}$. Provided $f(r)$ does not vary appreciably from unity in the vicinity of the wall, the constant, $c(\lambda)$, is of much the same character as the 'modified Oseen' constant introduced in § 7; its value can be determined afterwards in the usual fashion. The foregoing arguments give us a great deal of freedom in the selection of $f(r)$, since it is apparent that the r dependence is of little importance in the cell interior in either the high- or low-λ limit, provided $f(r)$ is nowhere too highly singular. In the intermediate-λ range we hope wise averaging procedures for the constant, $c(\lambda)$, will keep departures from the non-linearized solutions to a minimum.

One then wishes to choose an $f(r)$ which facilitates the mathematical analysis. One choice is $f(r) = 1/r$, since our solutions take the simple form $\Phi_i = r^{m_i}X(\theta)$ and $\Psi_i = r^{n_i}Y(\theta)$. Equations (2.16$b$) and (2.17$b$), when linearized in this manner, become

$$\eta\nabla^2\nabla^2\Psi - \frac{c}{r^2}\frac{\partial \nabla^2\Psi}{\partial\theta} = \eta\lambda\left(\cos\theta\frac{\partial}{\partial r} - \frac{\sin\theta}{r}\frac{\partial}{\partial\theta}\right)\Phi \tag{8.1}$$

and

$$\nabla^2\Phi - \frac{c}{r^2}\frac{\partial\Phi}{\partial\theta} = 0. \tag{8.2}$$

where the accompanying boundary conditions are given in (2.15). The r^{-1} behaviour will not lead to a divergence at the origin in the momentum equation provided each of the terms in (8.1) is either harmonic, represents a rigid-body rotation, or has its r dependence vanish at least as quickly as r^4 in the limit $r \to 0$. One can proceed with the solution and verify that these conditions are satisfied afterwards. Similarly, for the energy equation each of the terms in (8.2) vanishes at the origin provided Φ_i behaves as r^n, where $n \geqslant 2$. We shall find, when λ is sufficiently small, that the solution for Φ_i does pass through values for which $1 \leqslant n \leqslant 2$. However, if c is small compared to unity when this occurs, both terms in (8.2) are small everywhere in the domain of the problem except in the immediate neighbourhood of the origin; any errors should then be localized about this singular point for $c \ll 1{\cdot}0$.

Equation (8.2) has the general solution

$$\Phi = \sum_{m=1}^{\infty} a_m r^{n_m} e^{im\theta}, \tag{8.3}$$

where $n_m = m(1+ic/m)^{\frac{1}{2}}$ and m is integral since Φ must be periodic in θ. The solution is bounded at the origin if n_m is defined by its root in the second quadrant. The thermal boundary condition, $\Phi = \cos(\theta+\phi)$ at $r = 1$, is satisfied if all the $a_m = 0$ except when $m = 1$, in which case $a_1 = \alpha + i\beta$, where $\alpha = \cos\phi$ and $\beta = \sin\phi$. The temperature distribution is therefore described by the real part of

$$\Phi = (\alpha + i\beta) r^{n_1} e^{i\theta} \tag{8.4}$$

and is valid for all ϕ. It is convenient to write n_1 as

$$n_1 = A + iB = (1+c^2)^{\frac{1}{4}} \exp(\tfrac{1}{2} i \tan^{-1} c); \tag{8.5}$$

A and B are monotonically increasing functions of c. When $c < 6{\cdot}928$, $A < 2$, and the convective term in (8.2) indicates a physically non-realizable contribution at $r = 0$. In the next section we present an approximate variational solution, valid in the low-λ range corresponding to $A < 2$, which does have the proper behaviour at the origin. The solution for Φ, (8.3), is now substituted in equation (8.1). A separation-of-variables method can be used if one breaks the solution of the momentum equation into two successive steps, the first of which assumes that $\nabla^2\Psi$ is treated as the unknown. The mathematics is expedited by the independent-variable transformation, $\xi = \ln r$. Retaining only those modes in the general solution for Ψ that are the same as those introduced by the forcing terms, we find

$$\Psi/\lambda = a e^{2\xi} + b e^{2\xi + 2i\theta} + d e^{(n_1+3)\xi + 2i\theta} + f e^{(q+2)\xi + 2i\theta} + g e^{(n_1+3)\xi}, \tag{8.6}$$

where a, b and f are arbitrary complex constants, and d and g are the constant coefficients belonging to the particular solution, namely,

$$d = P/(Z_1 + iZ_2) \quad \text{and} \quad g = S/(Y_1 + iY_2), \tag{8.7}$$

where

$$2S = \alpha(A+1) - \beta B + i[\beta(A+1) + \alpha B], \quad 2P = \alpha(A-1) - \beta B + i[\beta(A-1) + \alpha B],$$

$$Y_1 + iY_2 = (n_1+1)^2 (n_1+3)^2 \quad \text{and} \quad Z_1 + iZ_2 = \left[(n_1+1)^2 - \left(4 + \frac{2ic}{\eta}\right)\right][(n_1+3)^2 - 4];$$

$q = 2(1+ic/2\eta)^{\frac{1}{2}}$ and is defined by its root in the second quadrant; thus

$$q = D+iE = 2(1+c^2/4\eta^2)^{\frac{1}{4}} \exp\{\tfrac{1}{2}i \tan^{-1}(c/2\eta)\}. \tag{8.8}$$

D and E are monotonically increasing functions of c; $D = 2$ and $E = 0$ at $c = 0$, their minimum values. Hence each of the terms in equation (8.1) satisfies the necessary criteria for boundedness established in the paragraph following (8.2). The general solution for Ψ, (8.6), will satisfy the boundary conditions at $\xi = 0$ if

$$a_r+ia_i = -\frac{n_1+3}{2}\frac{S}{Y_1+iY_2}, \quad b_r+ib_i = \frac{n_1-q+1}{q}\frac{P}{Z_1+iZ_2}$$

and

$$f_r+if_i = -\frac{n_1+1}{q}\frac{P}{Z_1+iZ_2}; \tag{8.9}$$

the subscripts r and i distinguish the real and imaginary parts of the complex constants in (8.6).

The expressions for the temperature distribution and stream function are the real parts of the complex solutions for Φ and Ψ, equations (8.4) and (8.6) respectively:

$$\Phi = r^A[\cos(B\ln r+\theta+\phi)], \tag{8.10}$$

$$\begin{aligned}\Psi/\lambda = {} & a_r r^2 + r^2(b_r\cos 2\theta - b_i \sin 2\theta) + r^{D+2}[f_r\cos(E\ln r+2\theta) - f_i\sin(E\ln r+2\theta)] \\ & + r^{A+3}[g_r\cos B\ln r - g_i\sin B\ln r + d_r\cos(B\ln r+2\theta) - d_i\sin(B\ln r+2\theta)].\end{aligned} \tag{8.11}$$

We shall evaluate the constant c later when we consider the evaluation of a similar constant in the 'cr' solution.

One can readily verify that (8.10) and (8.11) reduce to the Stokes flow solutions, $\Phi = r\cos(\theta+\phi)$ and $\Psi = \frac{1}{32}\lambda\cos\phi\,(\frac{1}{2}r^4 - r^2)$, in the limit $c \to 0$, provided $r \neq 0$. When $c \to \infty$, the 'c/r' solutions are related to the boundary-layer solutions, (7.8) and (7.9). Comparison of the two solutions establishes the relationship between the constants introduced for the linearizing velocity in each. The subscripts M and B will refer to the 'c/r' and the boundary-layer solutions, in that order. Since $r^\alpha = \exp(\alpha\ln r)$, and $\ln r = (r-1)-\frac{1}{2}(r-1)^2+\ldots$, $r^\alpha \approx e^{\alpha(r-1)}$ when $\alpha \gg 1$. Equations (8.10) and (8.11) can, therefore, be written when $\phi = \frac{1}{2}\pi$ as

$$\Phi_M = -\exp\{(\tfrac{1}{2}c_M)^{\frac{1}{2}}(r-1)\}\sin[(\tfrac{1}{2}c_M)^{\frac{1}{2}}(r-1)+\theta] \tag{8.12}$$

and

$$\begin{aligned}\Psi_M = {} & -\frac{\lambda r^2}{4c_M}\left[1 - \frac{\eta}{\eta-2}\left(\frac{2}{\sqrt{2}}-\sqrt{2}\right)\sqrt{\frac{\eta}{c_M}}\cos\left(2\theta+\frac{3\pi}{4}\right)\right] \\ & -\frac{\lambda}{2c_M^{\frac{3}{2}}}\left\{\exp\{(\tfrac{1}{2}c_M)^{\frac{1}{2}}(r-1)\}\left[\cos\left((\tfrac{1}{2}c_M)^{\frac{1}{2}}(r-1)+\frac{3\pi}{4}\right)\right.\right. \\ & \left. + \frac{\eta}{\eta-2}\cos\left((\tfrac{1}{2}c_M)^{\frac{1}{2}}(r-1)+2\theta+\frac{3\pi}{4}\right)\right] \\ & \left. -\frac{\eta}{\eta-2}\sqrt{\frac{\eta}{2}}\exp\{(c_M/\eta)^{\frac{1}{2}}(r-1)\}\cos\left((c_M/\eta)^{\frac{1}{2}}(r-1)+2\theta+\frac{3\pi}{4}\right)\right\}\end{aligned} \tag{8.13}$$

in the limit $c_M \to \infty$. These last expressions are identical to the singular perturbation solutions, (7.8) and (7.9), if

$$c_M = (\eta\lambda)^{\frac{1}{2}}c_B \quad \text{and} \quad \Psi_M = (\eta\lambda)^{\frac{1}{2}}\Psi_B. \tag{8.14}$$

9. The '*cr*' solution

The 'c/r' linearization is probably the only Oseen-type linearization possessing a relatively simple exact solution. We have seen, however, that this solution gives rise to a spurious convective contribution at the origin in equation (8.2) when $c_M < 6{\cdot}928$. For $c_M \ll 1{\cdot}0$ this error is confined to the immediate neighbourhood of the origin since at points removed from this singular point one is, for all practical purposes, considering the equation $\nabla^2\Phi = 0$. Therefore, we seek another approximate method of solution valid only for the small range of λ in which the 'c/r' solution is inaccurate. This solution will be of particular value for the flow near λ_{cr} when $\phi = \frac{1}{2}\pi$. A variational method of solution is well suited for this region of interest, since λ is small and polynomial representations of low degree should be satisfactory approximations for both Φ and Ψ.† $\mathbf{V} = cr\boldsymbol{\theta}$ is the only linearizing velocity of the type $\mathbf{V} = cf(r)\,\boldsymbol{\theta}$ that permits the resulting fluid dynamic equations to be cast by standard methods in equivalent variational form. The physical basis for this linearizing velocity, which is properly behaved at the origin, is fundamentally the same as for the 'modified Oseen' linearization already discussed. Again we hope to minimize the differences between the linearized and exact solutions by choosing the constant, c, such that the overall momentum and energy transfer are correct. The appropriate linearized equations are

$$\eta\nabla^2\nabla^2\Psi - c\frac{\partial\nabla^2\Psi}{\partial\theta} = \eta\lambda\left(\cos\theta\frac{\partial}{\partial r} - \frac{\sin\theta}{r}\frac{\partial}{\partial\theta}\right)\Phi \tag{9.1}$$

and

$$\nabla^2\Phi - c(\partial\Phi/\partial\theta) = 0. \tag{9.2}$$

The solution to (8.2) which satisfies the thermal boundary condition, $\Phi = \cos(\theta+\phi)$ at $r = 1$, is of the form $\Phi = f(r)\,e^{i(\theta+\phi)}$; $f(r)$, a complex function, satisfies

$$f'' + \frac{1}{r}f' - \left(\frac{1}{r^2} + ic\right)f = 0, \tag{9.3}$$

with $f(0) = 0$ and $f(1) = 1$ as boundary conditions. The forcing term on the right-hand side of (9.1) will, therefore, generate a solution for the stream function which has the form $\Psi/\lambda = g(r) + h(r)\,e^{2i\theta}$; $g(r)$ satisfies

$$g^{\mathrm{iv}} + \frac{2}{r}g''' - \frac{1}{r^2}g'' + \frac{1}{r^3}g' = \frac{e^{i\phi}}{2}\left(f' + \frac{f}{r}\right), \tag{9.4}$$

subject to the boundary conditions $g'(0) = g'(1) = 0$. In addition, both g and $\nabla^2 g$ are bounded at the origin since there can be neither an accumulation of fluid nor source of vorticity at this point. Similarly, for $h(r)$,

$$\eta\left(h^{\mathrm{iv}} + \frac{2}{r}h'''\right) + \left(-\frac{9\eta}{r^2} + 2ic\right)h'' + \left(\frac{9\eta}{r^3} + \frac{2ic}{r}\right)h' - \frac{8ic}{r^2}h = \frac{\eta e^{i\phi}}{2}\left(f' - \frac{f}{r}\right), \tag{9.5}$$

where $h(0) = h'(0) = h(1) = h'(1) = 0$. Equation (9.3) permits an exact solution in terms of Hankel functions of imaginary argument. However, with a view to

† The author is indebted to G. F. Carrier for this suggestion.

obtaining approximate solutions to (9.4) and (9.5), it is more convenient to seek an approximate solution for $f(r)$ that is a polynomial in r whose coefficients are determined using a variational scheme.

Thus, instead of (9.3) and (9.5), we wish to determine those $f(r)$ and $g(r)$ for which the integrals

$$I = \int_0^1 \left[\tfrac{1}{2}rf'^2 + \frac{1}{2}\left(\frac{1}{r} + cir\right)f^2\right] dr \tag{9.6}$$

and

$$J = \int_0^1 \left[-\tfrac{1}{2}\eta r h''^2 + \left(-\frac{9\eta}{2r} + cir\right)h'^2 + \frac{4ic}{r}h^2 + \tfrac{1}{2}\eta e^{i\phi}(rf' - f)h\right] dr \tag{9.7}$$

are stationary in value. Truncated series approximations for $f(r)$ and $h(r)$ which satisfy the boundary conditions and adequately describe the low-λ behaviour are

$$f(r) = r + A_1(r - r^2) + A_2(r - r^4) + A_3(r - r^6) \tag{9.8}$$

and

$$h(r) = r^2(1-r)^2(B_1 + B_2 r^2 + B_3 r^4), \tag{9.9}$$

respectively. The higher powers of r should pick out some of the features characteristic of the transition to the high-λ behaviour, although a series representation suitable for the entire λ spectrum would require many more terms than are used here. I and J are minimized and the approximations for $f(r)$ and $h(r)$ optimized if $\partial I/\partial A_i = 0$ and $\partial J/\partial B_i = 0$, $i = 1, 2, 3$. Once the integrals, (9.6) and (9.7), are evaluated these last conditions provide two sets of linear algebraic equations to determine the A's and B's. Equation (9.4) is an Euler differential equation and can be solved exactly. Denoting the real and imaginary parts of the coefficients by the subscripts r and i, respectively, and extracting the real parts of the solutions for Φ and Ψ, we obtain

$$\begin{aligned}\Phi = {} & [r + (A_{1r} + A_{2r} + A_{3r})r - A_{1r}r^2 - A_{2r}r^4 - A_{3r}r^6]\cos(\theta + \phi) \\ & - [(A_{1i} + A_{2i} + A_{3i})r - A_{1i}r^2 - A_{2i}r^4 - A_{3i}r^6]\sin(\theta + \phi)\end{aligned} \tag{9.10}$$

and

$$\begin{aligned}\Psi/\lambda = {} & D_{1r}r^2 + D_{2r}r^4 + D_{3r}r^5 + D_{4r}r^7 + D_{5r}r^9 + r^2(1-r)^2(B_{1r} + B_{2r}r^2 + B_{3r}r^4)\cos 2\theta \\ & - r^2(1-r)^2(B_{1i} + B_{2i}r^2 + B_{3i}r^4)\sin 2\theta,\end{aligned} \tag{9.11}$$

where the D's are the constant coefficients arising in the solution for $g(r)$. The temperature and velocity profiles which result are discussed in the next section.

The physical reasoning behind the selection of a suitable averaging criterion to determine the constant, c, in the 'c/r' and 'cr' solutions is basically the same as outlined in § 7, where we had to perform a similar procedure for the evaluation of the 'modified Oseen' constant. The only difference is that in the latter calculation we could average the equations over a region confined to the boundary layer, whereas in the present case the domain of integration includes the entire cell. The momentum and energy equations are coupled; therefore, the c *vs* λ relationship derived from one should not differ appreciably from the other. The simpler form of the energy equation will make its use the more convenient choice, other factors being equal. Because of the opposing symmetry properties of Φ and Ψ it is again necessary to weight equation (2.17) by a function of θ before the θ integration is performed. When $\phi = \frac{1}{2}\pi$ and λ is small we want the

weighting function to pick out not the actual temperature distribution, but the departure of our solution for Φ from the equilibrium solution, since it is just the differences between the two solutions which create the flow. Therefore, wanting to weight convective effects we multiply equation (2.17*b*) by $\cos\theta$. When $\phi = 0$,

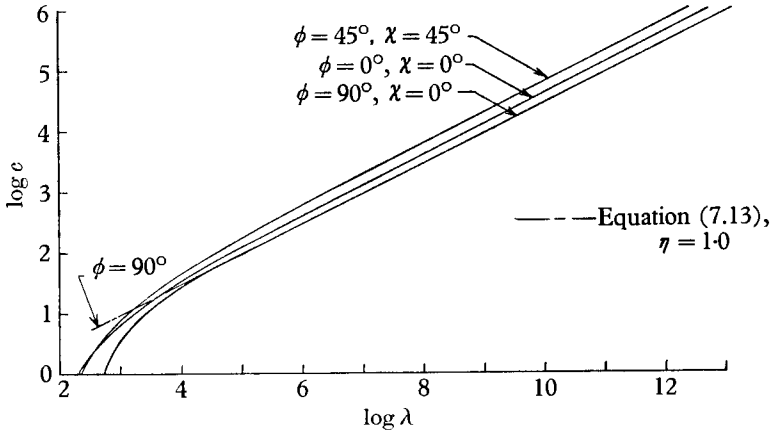

FIGURE 3. c *vs* λ curves for 'c/r' solution, $\eta = 1$.

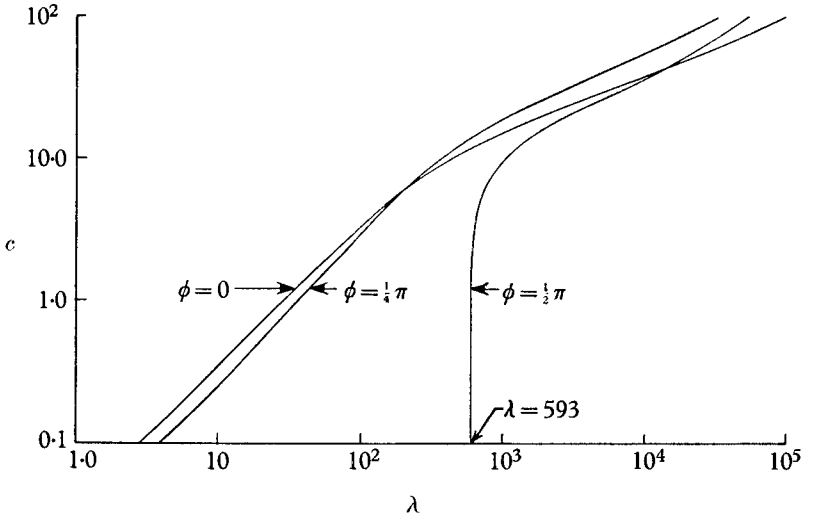

FIGURE 4. c *vs* λ curves for 'cr' solution, $\eta = 1$.

or $\phi = \frac{1}{4}\pi$, and there is no motionless state, we wish to emphasize the actual wall-temperature distribution. Hence $\cos\theta$ and $\cos(\theta + \frac{1}{4}\pi)$ are the appropriate weighting functions, in that order. Our criterion for determining c is then

$$\int_0^1 \int_0^{2\pi} \left[\nabla^2\Phi + \frac{1}{r}\left(\frac{\partial\Psi}{\partial r}\frac{\partial\Phi}{\partial\theta} - \frac{\partial\Psi}{\partial\theta}\frac{\partial\Phi}{\partial r}\right)\right] \cos(\theta + \chi)\, r\, dr\, d\theta = 0, \tag{9.12}$$

where the phase angle, χ, depends on which of the three cases is being considered.

For both the 'c/r' and 'cr' solutions the r- and θ-integrations in (9.12) can be performed analytically. The resulting solutions with $\eta = 1$ where obtained by

programming an IBM 7090 computer for our three situations of interest: $\phi = 0$, $\chi = 0$; $\phi = \frac{1}{4}\pi$, $\chi = \frac{1}{4}\pi$; $\phi = \frac{1}{2}\pi$, $\chi = 0$. The c *vs* λ curves obtained are shown in figures 3 and 4. Figure 3 provides a means of estimating the range of validity of boundary-layer solutions presented in § 7. If equation (7.13) is used in conjunction with (8.14) we obtain the dashed line shown in the figure. Departures in c from the results of the 'c/r' solution are confined to less than 10% for $\lambda > 5 \times 10^4$. We see from figure 4 that when $\phi = 0$ or $\frac{1}{4}\pi$ all velocities become vanishingly small as $\lambda \to 0$, whereas for $\phi = \frac{1}{2}\pi$ all motion ceases as $\lambda \to 593$. This value is within a few per cent of the value for λ_{cr} which our linear stability theory predicted in § 5.

10. Results

The 'c/r' and 'cr' solutions for the temperature distribution and velocity components were obtained by programming an IBM 7090 computer for representative values of c covering the entire λ spectrum for $\phi = 0$, $\frac{1}{4}\pi$, and $\frac{1}{2}\pi$. These

	λ		
c	$\phi = 0$	$\phi = \frac{1}{4}\pi$	$\phi = \frac{1}{2}\pi$
0·1	$2{\cdot}317 \times 10^1$	$3{\cdot}181 \times 10^1$	—
1·0	$1{\cdot}994 \times 10^2$	$2{\cdot}226 \times 10^2$	—
10	$1{\cdot}908 \times 10^3$	$1{\cdot}402 \times 10^3$	$2{\cdot}677 \times 10^3$
10^2	$7{\cdot}832 \times 10^4$	$4{\cdot}233 \times 10^4$	$1{\cdot}236 \times 10^6$
10^3	$6{\cdot}240 \times 10^6$	$2{\cdot}880 \times 10^6$	$1{\cdot}191 \times 10^7$
10^4	$5{\cdot}890 \times 10^8$	$2{\cdot}558 \times 10^8$	$1{\cdot}257 \times 10^9$
6·928	$1{\cdot}19 \times 10^3$	$9{\cdot}36 \times 10^2$	$1{\cdot}70 \times 10^3$

TABLE 1. Representative values of c and λ, 'c/r' solution.

	λ		
c	$\phi = 0$	$\phi = \frac{1}{4}\pi$	$\phi = \frac{1}{2}\pi$
0·1	$2{\cdot}814 \times 10^0$	$3{\cdot}951 \times 10^0$	$5{\cdot}932 \times 10^2$
1·0	$2{\cdot}829 \times 10^1$	$3{\cdot}732 \times 10^1$	$5{\cdot}986 \times 10^2$
10	$4{\cdot}372 \times 10^2$	$3{\cdot}569 \times 10^2$	$1{\cdot}037 \times 10^3$
20	$1{\cdot}923 \times 10^3$	$1{\cdot}094 \times 10^3$	$2{\cdot}870 \times 10^3$
50	$2{\cdot}076 \times 10^4$	$7{\cdot}787 \times 10^3$	$1{\cdot}801 \times 10^4$
100	$1{\cdot}003 \times 10^5$	$3{\cdot}355 \times 10^4$	$5{\cdot}567 \times 10^4$

TABLE 2. Representative values of c and λ, 'cr' solution.

results and their region of overlap with the Stokes flow and singular perturbation solutions are presented and interpreted in this section and compared with experimental observations whenever possible. Having already determined the cell behaviour as a function of η for those situations where it is physically interesting, namely the high-λ limit of the $\phi = \frac{1}{2}\pi$ case, we limit the present discussion to $\eta = 1$, a convenient representative value. When $\phi = 0$ the Prandtl number has little influence on the interior motion in the high-λ limit since, as we shall see shortly, $\omega_0 \to 0$ as $\lambda \to \infty$ for all η.

The solutions for the temperature and velocity profiles were obtained for $c = 0{\cdot}1$, 1·0, 10, 10^2, 10^3, and 10^4 for the 'c/r' solution and for $c = 0$, 1, 1·0, 10, 20, 50, and 100 for the 'cr' solution. The corresponding values of λ are given for

easy reference in tables 1 and 2. Table 1 includes the values of λ for which $c = 6{\cdot}928$, the point at which the 'c/r' solution diverges at the origin.

Figures 5 and 6, plots of equations (8.10) and (9.10), respectively, show temperature profiles for various values of c at the angular position for which the

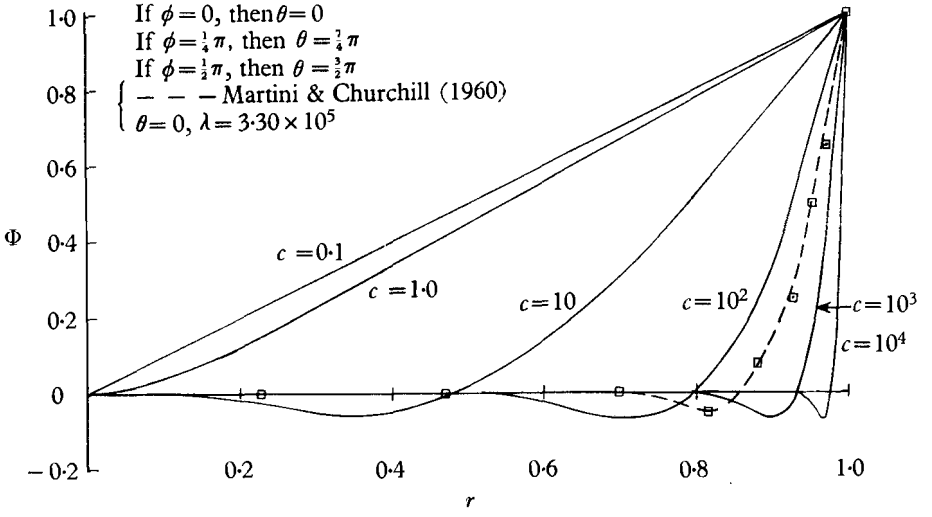

FIGURE 5. Temperature profiles at position of maximum wall temperature for 'c/r' solution.

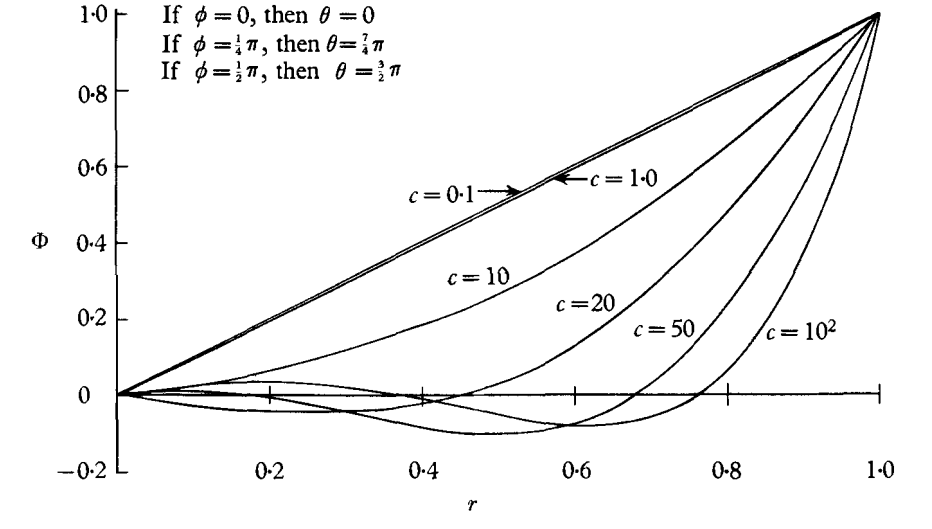

FIGURE 6. Temperature profiles at position of maximum wall temperature for 'cr' solution.

wall temperature is maximum. The same curves apply to all three cases of interest if we adjust properly for phase differences. This does not imply that for a given λ all three cases have geometrically similar temperature distributions; the c *vs* λ curves differ, of course, for each. The dominant characteristic one notices is the formation of a constant temperature interior and thermal boundary layer

as λ increases. A secondary feature is the tendency of the temperature profiles to overshoot the $\Phi = 0$ value at the edge of the core region. This is a convective response to a primary convective effect which displaces hot and cold fluid elements by 90 degrees. The dashed curve in figure 5 was obtained from the experimental data of Martini & Churchill (1960). Their thermal boundary condition (left- and right-hand halves of their cylinder are maintained at constant but different temperatures) differs in detail but is qualitatively similar to our $\phi = 0$ case. Based on figure 3, $c \approx 250$ for the Rayleigh number at which they conducted their test.

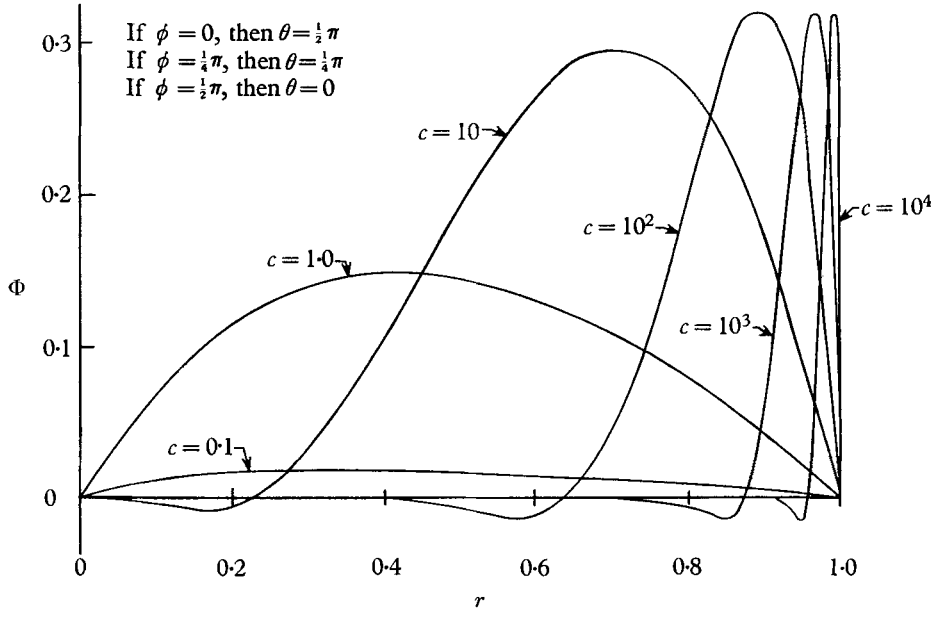

FIGURE 7. Temperature profiles 90 deg counterclockwise from position of maximum wall temperature for 'c/r' solution.

Proceeding 90 deg counter clockwise from the position of maximum wall temperature, we obtain the temperature profiles shown in figure 7. The convective motion carries the hot fluid from the heated side through a quarter of a circle creating a region of relatively warm fluid at the θ position where $\Phi = 0$ at the wall. Since $\Phi(r, \theta) = -\Phi(r, \theta + \pi)$, a similar region of comparatively cool fluid forms diametrically opposite the position for which the curves of figure 7 apply. As λ increases these hot and cold regions move radially outward increasing the effective torque on the interior portion of the cell due to the increased lever arms about the origin of these hot and cold regions. For all ϕ other than $\phi = 0$ this couple acting at the edge of the interior region causes the core to rotate as a solid body, the net moment being greatest when $\phi = \frac{1}{2}\pi$. When $\phi = 0$ the heated and cooled fluid elements rest at the top and bottom of the cell, respectively, in a stabilizing manner. The component of the buoyancy couple which produces the core rotation when $\phi \neq 0$ now vanishes, and instead one finds a stabilizing torque that resists such a rotation and which, we shall see,

virtually arrests the interior motion when λ is sufficiently large. Figure 8 provides a more detailed description of the thermal boundary-layer structure for a representative high-λ situation, $c = 10^3$. Successive boundary-layer temperature profiles, taken at θ stations 22·5 deg apart, display the manner in which a region of relatively warm fluid is established adjacent to a wall station where $\Phi = 0$.

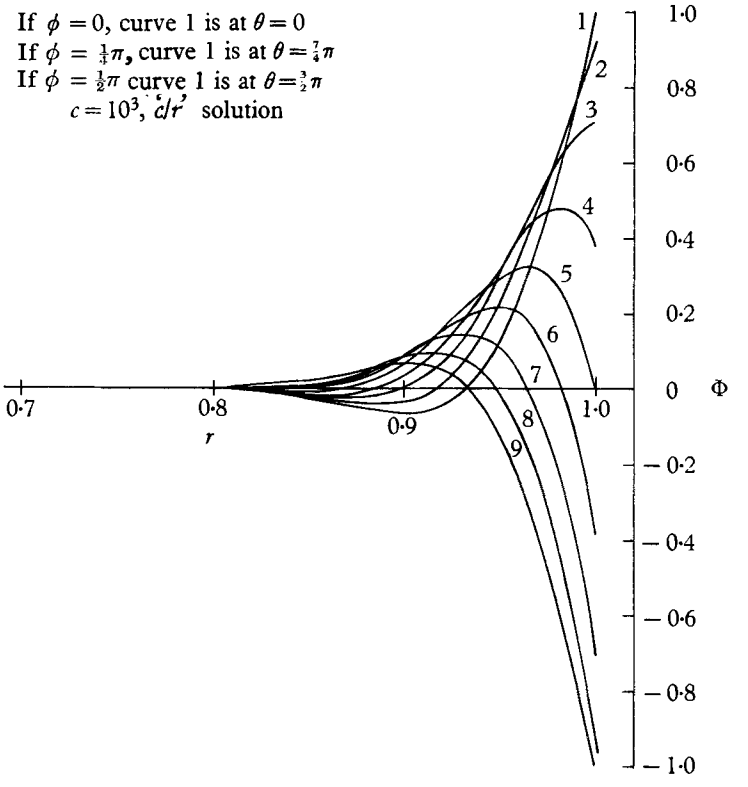

FIGURE 8. Boundary-layer temperature profiles at various θ positions for a representative high-λ situation. Curve 1 is taken at the angular position of maximum wall temperature and each succeeding curve is 22·5 deg counterclockwise from the previous one.

Regardless of the choice of ϕ or c, the machine-computed results indicate that V_r is at most an order of magnitude less than V_θ everywhere within the domain of the cell. The normalized velocity profiles we discuss next, therefore, are based on V_θ. They are obtained from equations (8.11) and (9.11). Figures 9 and 10 refer to our $\phi = 0$ arrangement. The normalized velocity profiles when $c = 0{\cdot}1$ in both figures are each very nearly identical to those obtained from the Stokes-flow theory. Based on the 'cr' solution, departures of more than 1 % from the Stokes-flow velocity profiles are first noticed for $\lambda \approx 50$. As deduced from the temperature profiles for the $\phi = 0$ case, one observes, with increasing λ, a progressive stagnation of the core and the creation of a narrow circulating fluid layer adjacent to the wall. The core behaves much as if it were disk weighted at its bottom. At high values of λ the shearing moment exerted on the interior by the convecting fluid in the boundary layer is not sufficient to overcome the stabilizing

influence of the buoyancy couple acting on the interior region. Velocity profiles for the convecting fluid band are shown at various θ positions for a representative high-λ situation in figure 11. A fluid element in the circulating ring is accelerated

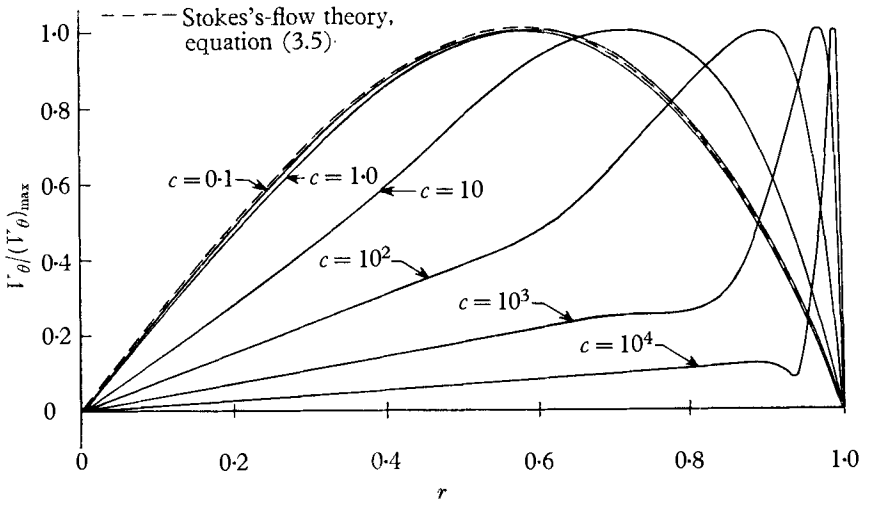

FIGURE 9. Velocity profiles when $\phi = 0$ at $\theta = 0$ from 'c/r' solution, $\eta = 1$.

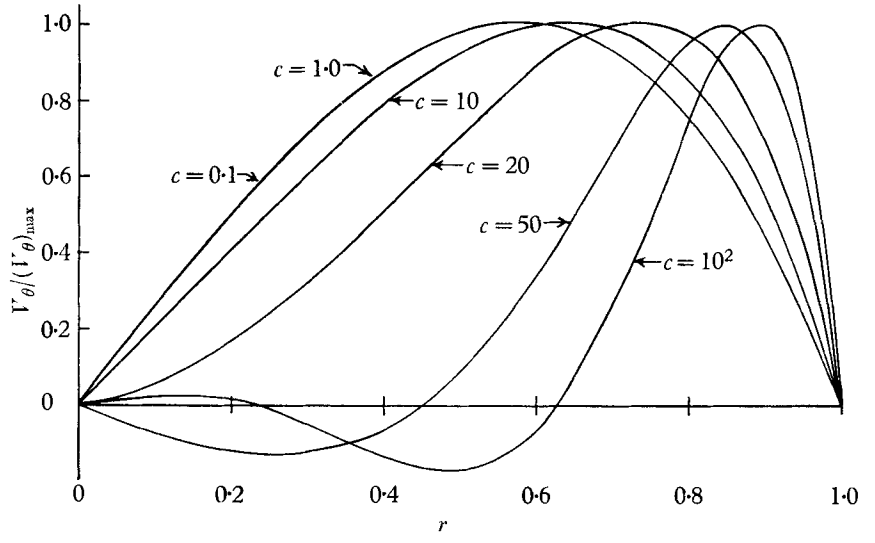

FIGURE 10. Velocity profiles when $\phi = 0$ at $\theta = 0$ from 'cr' solution, $\eta = 1$. The curves for $c = 0{\cdot}1$, $1{\cdot}0$ and the Stokes-flow theory, equation (3.5), cannot be distinguished using the above scale.

by buoyancy forces in advancing from positions 1 to 5. Conservation of mass requirements prevent the boundary layer from thickening along this segment of the periphery. In passing over the top and proceeding down the cold wall toward $\theta = \pi$, the rotating fluid band experiences a stabilizing density gradient. The effect is to both retard the fluid motion in and increase the width of the

convecting band. Since Ψ' is centro-symmetric the boundary-layer behaviour just described repeats itself when we complete the circuit along the bottom half of the cylinder. All the interior and boundary-layer motions which we have described have been observed by Martini & Churchill in their experiments. At the highest Rayleigh numbers for which they conducted their tests, $\lambda \approx 10^7$,

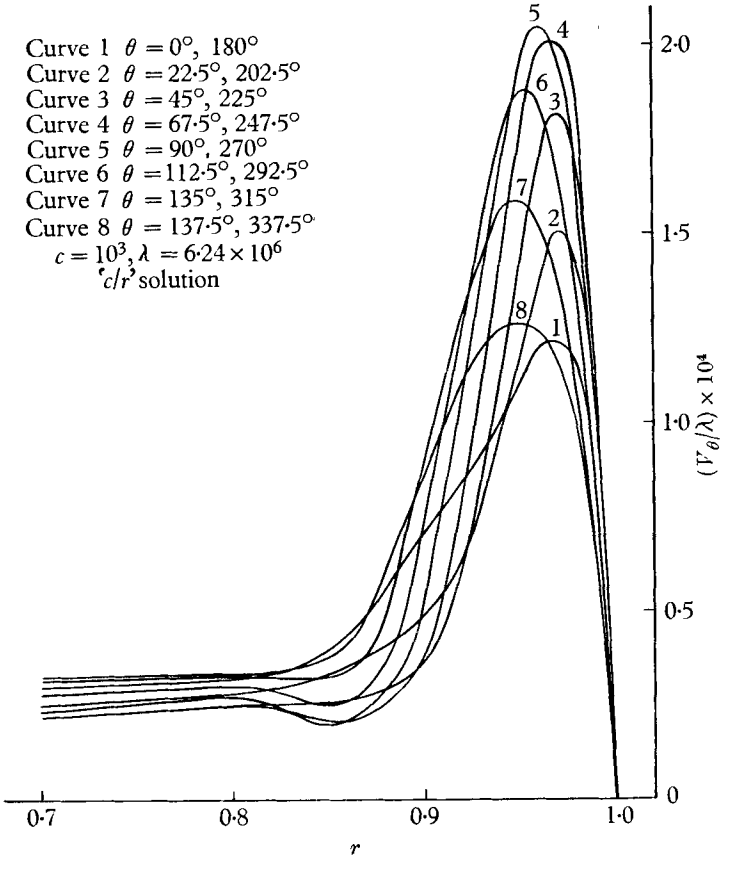

FIGURE 11. Boundary-layer velocity profiles for $\phi = 0$ case at θ intervals of 22·5 deg for a representative high-λ situation, $\eta = 1$.

all motions were still two-dimensional, with no evidence of either the onset of turbulence or the presence of Taylor instabilities. It is apparent from the preceding discussion why an Oseen singular-perturbation method of solution, which assumes a rotating solid-core behaviour, is unsuccessful for the $\phi = 0$ case. The core vorticity, which is a non-zero constant in the high-λ limit, for all ϕ other than $\phi = 0$, vanishes when $\phi = 0$.

The normalized velocity profiles for the $\phi = \frac{1}{2}\pi$ cases are plotted in figures 12 and 13. The '*cr*' solution provides the more accurate description for the motion near the critical Rayleigh number, whereas the '*c*/*r*' solution is more reliable for λ greater than roughly 10^4. For the very slow motion near λ_{cr} the velocity profiles differ from the Stokes-flow profiles for the $\phi \neq \frac{1}{2}\pi$ cases in that the position of

maximum velocity is shifted toward the origin. As anticipated, a rigid rotating-core motion is manifested at high values of λ. The velocity profiles are slightly peaked at the edge of the cell interior due to the thermal overshoot that occurs in this region. The overshoot creates a clockwise moment on the interior region which must be balanced by an opposing shearing moment if the core is to rotate with constant angular velocity and experience a zero net torque.

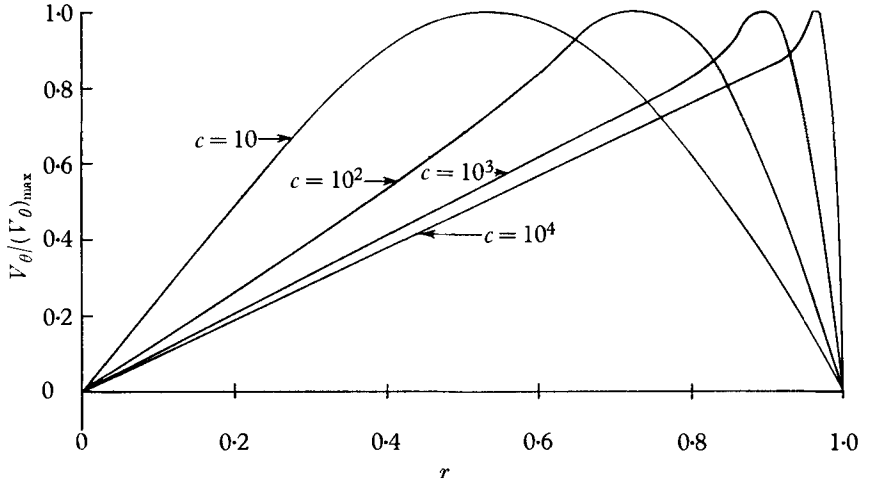

FIGURE 12. Velocity profiles when $\phi = \frac{1}{2}\pi$ at $\theta = \frac{3}{2}\pi$ from 'c/r' solution, $\eta = 1$.

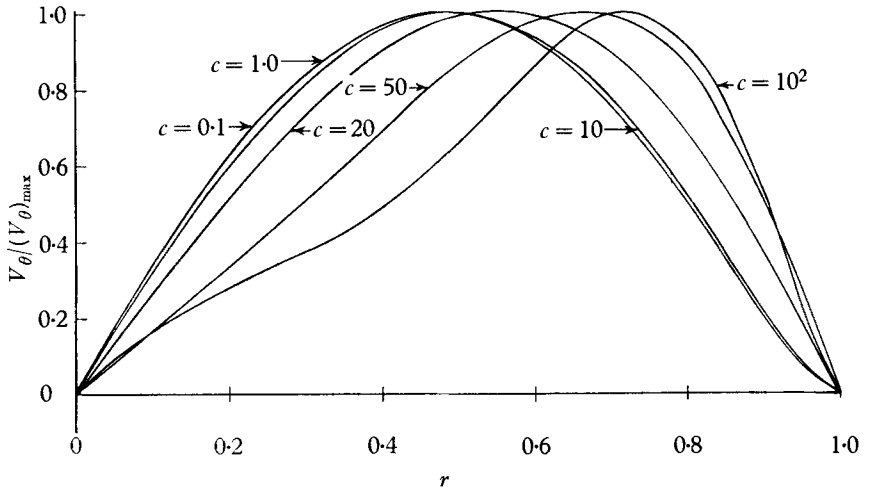

FIGURE 13. Velocity profiles when $\phi = \frac{1}{2}\pi$ at $\theta = \frac{3}{2}\pi$ from 'cr' solution, $\eta = 1$.

Figure 14 shows that the $\phi = \frac{1}{4}\pi$ case is a hybrid phenomenon whose solution contains elements of each of the $\phi = 0$ and $\frac{1}{2}\pi$ solutions. This solution exhibits the Stokes-flow behaviour characteristic of the $\phi = 0$ case when λ is small and the rigid rotating-core behaviour we find for the $\phi = \frac{1}{2}\pi$ case when λ is large. Only the $\phi = \frac{1}{2}\pi$ case has a motionless equilibrium configuration at the low end of the λ spectrum, and only the $\phi = 0$ case has a self-stabilizing core for high values

of λ. Thus, the qualitative behaviour of the $\phi = \frac{1}{4}\pi$ case is representative of all ϕ except the special cases $\phi = 0$ and $\frac{1}{2}\pi$. Finally, we need a uniform criterion to establish both the region of validity and overlap of the different solutions pre-

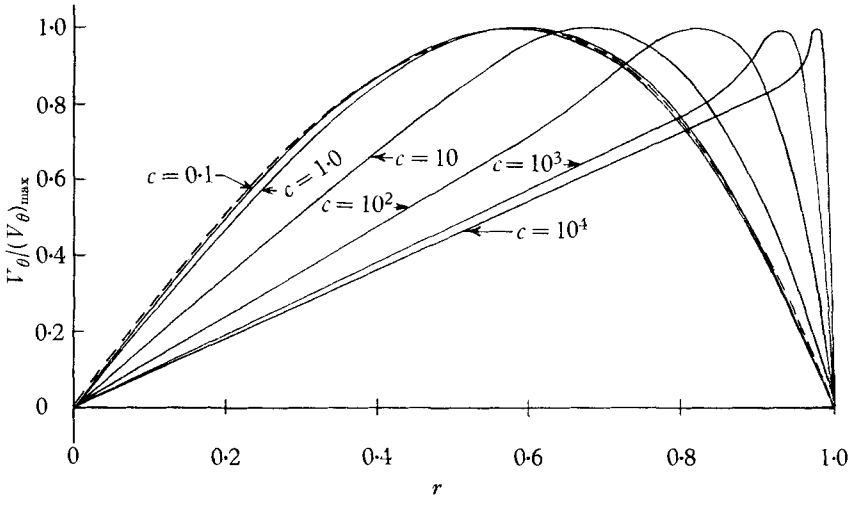

FIGURE 14. Velocity profiles when $\phi = \frac{1}{4}\pi$ at $\theta = \frac{3}{4}\pi$ from 'c/r' solution, $\eta = 1$. — —, Stokes's flow theory, equation (3.5).

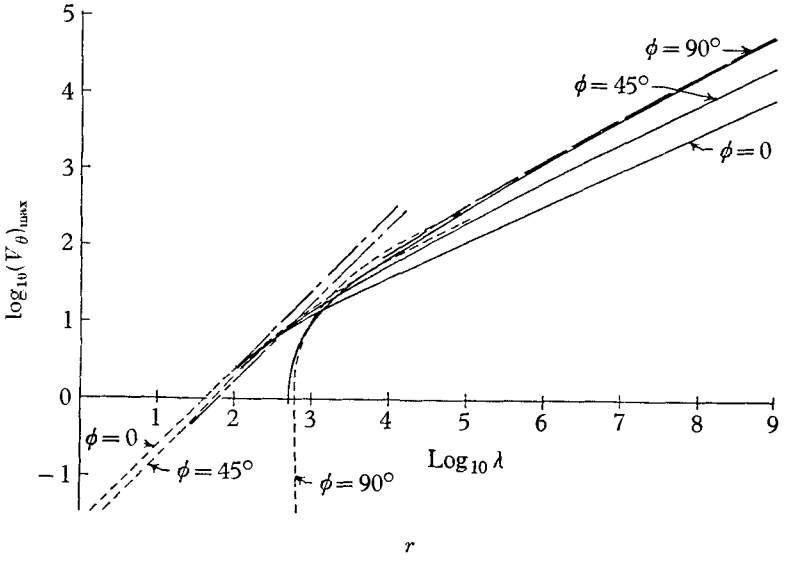

FIGURE 15. $(V_\theta)_{max}$ *vs* λ for $\phi = 0$, $\frac{1}{4}\pi$, and $\frac{1}{2}\pi$. $(V_\theta)_{max}$ as used here refers to the maximum value of V_θ at the angular position of maximum wall temperature. ——, Exact 'c/r' linearization; — —, boundary-layer solution; – – – –, 'c/r' variational method; — — —, Stokes's-flow theory; $\eta = 1{\cdot}0$.

sented. Curves of $(V_\theta)_{max}$ *vs* λ, with $\eta = 1$, are plotted in figure 15 for this purpose and are self explanatory. In the low-λ limit $(V_\theta)_{max} \propto \lambda$ except when $\phi = \frac{1}{2}\pi$ in which case $(V_\theta)_{max} \to 0$ as $\lambda \to 593$. The curves, having passed through the inter-

mediate-λ transition region, then asymptote to a high-λ behaviour in which $(V_0)_{\max} \propto \lambda^{\frac{1}{2}}$ for all ϕ.

The author wishes to acknowledge the guidance and inspiration of his thesis advisor Prof. George F. Carrier, of Harvard University, under whose supervision this work was conducted.

The material in this paper is based on the author's Ph.D. thesis which was submitted to the Division of Engineering and Applied Physics at Harvard University, Cambridge, Massachusetts; it is also available in unabridged form as Sperry Rand Research Center Report no. 63-14.

REFERENCES

BATCHELOR, G. K. 1954 Heat transfer by free convection across a closed cavity between vertical boundaries at different temperatures. *Quart. Appl. Math.* **12**, 209.

BATCHELOR, G. K. 1956 On the steady laminar flow with closed streamlines at large Reynolds number. *J. Fluid Mech.* **1**, 177.

BÉNARD, H. 1900 The cellular motion in a liquid layer transporting heat by convection in a steady regime. *Rev. Gen. Sci. Pur. Appl.* **12**, 1261.

CARRIER, G. F. 1953 Boundary layer problems in applied mathematics. *Adv. Appl. Mech.* **3**, 1.

LEWIS, J. A. 1950 Free convection in commercially insulating materials. Ph.D. thesis, Brown University, Providence, R.I.

MARTINI, W. R. & CHURCHILL, S. W. 1960 Natural convection inside a horizontal circular cylinder. *A.I.Ch.E. J.* **6**, 251.

PELLEW, A. & SOUTHWELL, R. V. 1940 On maintained convection motion in a fluid heated from below. *Proc. Roy. Soc.* A, **176**, 312.

PILLOW, A. F. 1952 The free convection cell in two dimensions. *Aust. Dep. Supply Aero. Res. Lab., Rep.* A 79.

RAYLEIGH, LORD 1916 On convection currents in a horizontal layer of fluid, when the higher temperature is on the upper side. *Phil. Mag.* **32**, 529.

SCHMIDT, R. & SAUNDERS, O. 1937 On the stability of a fluid when heated from below. *Proc. Roy. Soc.* A, **165**, 216.

SEGEL, L. A. & STUART, J. T. 1962 On the question of the preferred mode in cellular thermal convection. *J. Fluid Mech.* **13**, 289.

WEINBAUM, S. 1963 Ph.D. thesis, Harvard University, Cambridge, Mass.